Dark Cosmology Centre
Niels Bohr Institute
Copenhagen University

Spectral Energy Distributions of Gamma Ray Burst Host Galaxies

Master Thesis

Michał Michałowski

Supervisor: Prof. Jens Hjorth

Copenhagen 2006

Abstract

This Master Thesis is concentrated on the fitting of the Spectral Energy Distribution (SED) templates to the broad-band observational data of Gamma Ray Bursts (GRB) host galaxies, which were bright in submillimetre and/or radio wavelengths, namely hosts of GRB 980703, GRB 000210, GRB 000418 and GRB 010222. This is the first successful entire SED fitting, from optical to radio wavelengths, achieved for GRB hosts. I present constraints on their properties, including the need for high dust temperatures, high star formation rates (SFR) and low ages. I estimated very conservative and robust lower limits on the dust temperatures in a range from $T \gtrsim 29$ K to $T \gtrsim 59$ K. Their SFRs derived from infrared emission range from 179 to 1211 solar masses per year and it places GRB hosts in a category of highly star-forming galaxies. I propose that the seeming contradiction of high SFRs and blue optical colors of GRB hosts can be explained by their low ages in a range from 90 Myr to 2 Gyr.

Contents

Acknowledgments

First and foremost, I would like to express my deep gratitude to Joanna Baradziej for her constant help, support and understanding during the writing of this thesis. Because of their wonderful attitude I was able to finish the work and I would like to dedicate this Master Thesis to her.

My research on Gamma Ray Bursts Hosts would have never started without my supervisor Jens Hjorth. He introduced me to the field of GRBs, when I didn't basically know anything about them except of limited knowledge acquired during one of the Bohdan Paczyński's lecture in Toruń. I am extremely grateful to Jens for always being friendly, having lots of valuable answers, comments, advice and new ideas each time I came into his office.

I want to thank bunch of people who had inestimable influence on my work: José María Castro Cerón for fruitful collaboration; Darach Watson for numerous discussions and for showing me the powerful `GRASIL` code; Frank Bertoldi and Mike Garrett for useful comments and for drawing my attention on far infrared-radio correlation; Brad Cavanagh, Frossie Economou, Tim Jenness, Carsten Skovmand for one-year-long successful struggle with my `ORAC-DR` installation; and David Elbaz for kindly providing the observed SEDs of Arp 220 and HR 10.

I wish to thank José María Castro Cerón, Tamara Davis, Árdís Elíasdóttir, Signe Riemer-Sørensen and Max Stritzinger for the time spent on proofreading of this thesis. Without you, it would contain countless number of mistakes such as wrong usage of never-understandable *a* and *the*.

It was really great to share the office with Desiree Della Monica Ferreira, Peter Laursen and Signe Riemer-Sørensen. Thanks for friendly atmosphere and for speaking in Danish to me. I also appreciate wonderful working and social environment in the Dark Cosmology Centre. Thanks for discussions, astro-ph coffees, parties, etc. Special thanks to Janaki Bettina Lund Jensen for administrative help and Brian Lindgren Jensen for help with computers and for writing an excellent Master Thesis (Jensen 2004), which provided numerous useful references to the literature relevant to my work.

I am also so grateful to my family: my Mum, Dad, Anita, Jurek and

Paweł for all that they have done for me and my friends in Poland for patient waiting for my arrival.

Finally, I would like to acknowledge the support from the Socrates/Erasmus Scholarship, Polish Ministry of Education and Science Scholarship, Danish Governmental Scholarship, Stefan Rozental og Hanna Kobylinski Rozentals Fond, as well as Niels Bohr Institute and Dark Cosmology Centre for financing my conferences and summerchools travels.

Michał Michałowski

Copenhagen, 13.08.2006

Chapter 1

Introduction

Gamma Ray Bursts (GRBs) had remained a mystery for more than 30 years after the first detection and still provide unexpected clues that change our view on these events. In Chapter 2 I introduce the observational facts and the physics of GRBs, which provide an explanation of why GRBs are worth studying and, in turn, why the research presented in this thesis is valuable for development of the cosmology. It is because they are so bright that can be used in many aspects of the entire Universe studies.

One of the important aspects of GRB studies is the nature of their host galaxies. The present status of our knowledge of this population of galaxies is described in Chapter 3. I also highlight the motivation of this work, which aim to discuss the issue of Spectral Energy Distributions (SEDs) of GRB host galaxies. It has not been investigated previously for entire wavelength range, so I make an attempt to do it for a first time. It is important, because SEDs provide firm estimation of Star Formation Rates, which can bridge the GRBs with the aspect of star formation in the Universe as well as they enable us to constrain many characteristics of the host galaxies necessary to investigate the environment of GRB progenitors.

This thesis is dealing with somewhat striking observational results for four GRB hosts: GRBs 980703, 00210, 000418 and 010222. They are the only hosts detected, up to date, either in submm and/or radio, indicating high star-forming/dusty galaxies. On the other hand, their blue colours are consistent with little or no dust and moderate star-formation activity. In Chapter 4 I present my own reduction of SCUBA data leading to detections of the hosts mentioned before. The reason to re-reduce the data is to confirm that they are not just artefacts connected with noise and/or reduction process.

The main part of this thesis tries to resolve of the discrepancy between submm/radio and optical observations by means of fitting SED templates to

the broad-band data. This multi-wavelength approach gives the possibility to include all available data simultaneously. Having fitted these functions I aim to derive many of the characteristics of the GRB hosts in a more robust way than in those studies restricted only to certain wavelengths.

In Chapter 5 I apply the analytical SED modelling to the long-wavelength observations of the hosts and attempt to constrain properties of the dust present in these galaxies.

I include all the data available in the literature, from optical to radio, in Chapter 6 and fit different SED templates, ranging from quiescent to starburst galaxies, in order to check to which category of galaxies GRB hosts belong to.

Chapter 7 contains the (first ever) fitting of the entire SEDs of the GRB hosts. The goal is to construct a template that represents both optical and submm/radio observations simultaneously.

All three approaches to SEDs (Chapter 5, 6 and 7) give the possibility to estimate the SFRs of the hosts. I aim to compare these values with those derived from optical indicators and analyse them in the context of different galaxy samples established in optical/infrared/submm/radio surveys.

Finally in Chapter 8 I summarise this work, highlight the main results and propose the future research in this subject.

Unless explicitly noted, GRBs mentioned are long GRBs with durations longer than 2 s. Throughout I apply the cosmology characterised by $\Omega_m = 0.3$, $\Omega_\Lambda = 0.7$, $H_0 = 72$ km/s/Mpc.

Chapter 2

Gamma Ray Bursts

2.1 First Observations

Gamma Ray Bursts (GRBs) are intense transient events of γ-ray emission with energies of $E > 10^5$ eV corresponding to wavelengths of $\lambda < 0.01$ nm. A burst can last from a few milliseconds to several minutes. It overshines all other γ-ray sources and then fades away. It is followed by decaying emission in other wavelengths (X-ray to radio) known as an afterglow. The observed rate of GRBs is approximately one per day.

Since the Earth's atmosphere absorbs γ-ray photons, GRBs can only be observed from space with satellites. They were first detected in 1967 by the U.S. Air Force military satellite *Vela*, while looking for γ-ray emission which could indicate nuclear tests performed by the Soviet Union. The first detections were reported a few years later by Klebesadel et al. (1973).

In the early 1990s there was a debate among astronomers whether GRBs had Galactic or extra-Galactic origin. Finally, as reported by Paczyński (1991), the Burst and Transient Source Experiment (BATSE) on board of the Compton Gamma-Ray Observatory (CGRO) revealed the uniform distribution of GRBs on the sky as shown in Figure 2.1 (Greiner 1999). Meegan et al. (1992) and Briggs (1995) reported only 0.9σ and 0.3σ deviation from complete isotropy in terms of dipole and quadrupole distributions, respectively. This supported the hypothesis of cosmological distances to GRBs. If GRBs were located in the Milky Way they would be preferentially distributed on the Galactic plane or concentrated towards the Galaxy center similar to halo objects (Paczyński 1995).

An extragalactic origin of GRBs was confirmed when the first spectrum of the afterglow (see Section 2.4) of GRB 970508 was taken and a redshift[1]

[1] Redshift is a cosmological way to measure distances and is equal to ratio of the spectral

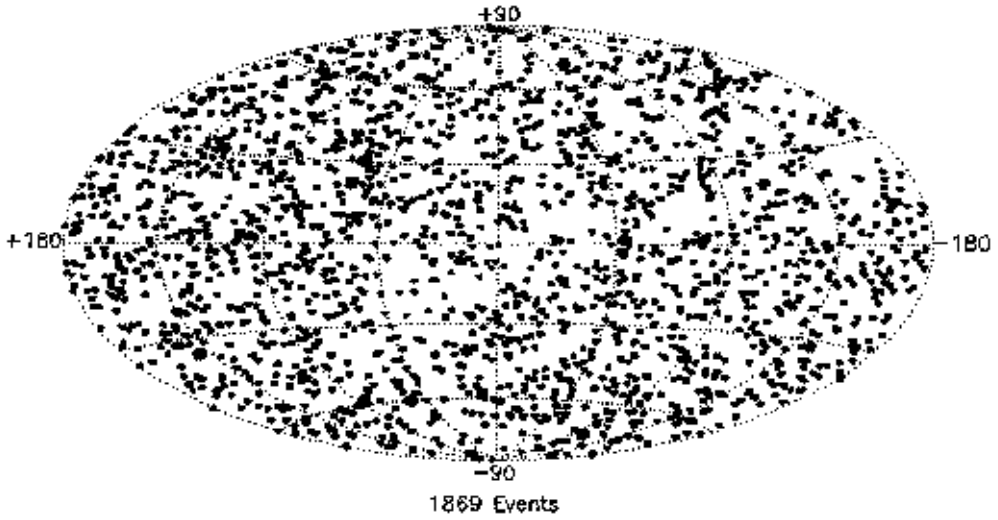

Figure 2.1: Distribution of GRBs on the sky. Uniformity is the argument in favour of their extragalactic origin (Greiner 1999).

of $z = 0.835$ was measured (Metzger et al. 1997). The most distant GRB observed to date (summer 2006) was GRB 050904 at the redshift of $z = 6.3$ (Tagliaferri et al. 2005). It exploded when the Universe was only 840 million years old (i.e. 6.4% of the present age).

2.2 GRB Event

The brightness of prompt GRB emission is quantified by the so-called fluence — the flux integrated over the duration of the burst measured in the energy bin $\sim 10 - 100$ keV. Typically it has a value of $\sim 10^{-4} - 10^{-6}$ erg/cm^2. The energy of emitted photons ranges between 1 and 1 000 keV, but some GRBs emit photons with even higher energy i.e. 100 MeV $-$ 20 GeV delayed with respect to the low-energetic photons (Fishman & Meegan 1995). More energetic photons have not been detected yet, but those with energies of 20 GeV $-$ 1 TeV are expected to be emitted during the GRB event (Poirier et al. 2003).

Spectra of GRB prompt emissions are non-thermal with a power-law distribution of energy. A more detailed analysis revealed that all the GRB

shift in wavelength $\Delta\lambda$ to the value of wavelength λ: $z = \Delta z/z$. For long distances this shift is dominated by cosmological expansion and the distance to the object can be estimated via the Hubble law.

spectra can be described at low energies by a power-law with an exponential cut-off $N(E) \propto E^{-\alpha} \exp(-E/E_0)$ and at high energies by a steeper power-law $N(E) \propto E^{\beta}$ with $\alpha < \beta$ (Band et al. 1993). It was found that $\alpha \sim 1$, $\beta \sim 2 - 3$ and the break energy $E_0 \sim 100$ keV $- 1$ MeV with most of the burst having $E_0 < 200$ keV (Band et al. 1993).

The total energy released by a GRB can be as high as 10^{54} erg and typically not less than 10^{52} erg. It corresponds to the conversion into radiation the mass of more than one solar mass (Cheng & Lu 2001). This implies that GRBs are the most powerful events in the Universe. However, a natural way to avoid such a high energy release is to assume that γ-ray emission is beamed (see Section 2.4). Then the total burst energy is still high, but at a lower value equal $10^{50} - 10^{52}$ erg (Fargion 2001; Ghisellini 2001).

The γ-ray-lightcurves are complicated and have no standard morphology (see Figure 2.2). Substructures are sometimes resolved down to the millisecond time-scale and complicated spikes may be present. Others show fast increases of flux and subsequent nearly exponential decay. Some bursts are double, triple or more multiple.

In spite of their complexity some attempts have been made to make a general classification scheme for GRBs. According to Kouveliotou et al. (1993) there was a bimodal distribution of the burst duration (T): long GRBs with $T > 2$ s and short GRBs with $T < 2$ s (Figure 2.3). Long GRBs have been observed 3 times more than short GRBs. The hardness is also connected with duration: short bursts are harder (they emit more high-energy photons) compared to long bursts (Hurley et al. 1992; Kouveliotou et al. 1995).

The γ-ray emission is strongly variable with a variability scale $\delta T \sim 100$ times shorter than its duration (Cheng & Lu 2001). It can be used to derive an upper limit on the spatial scale of the source. The source cannot be bigger than $R < c\delta T \sim 300$ km ($\delta T = 1$ ms), where c is the speed of light. Otherwise, the signals from the opposite regions, casually disconnected during the variability time scale, would cancel out the variations. Even if we assume that there is a black hole in this boundary its mass is $M < c^2 R/2G \sim 100 M_{\odot}$, where G is the gravitational constant and $M_{\odot}$ is the solar mass. Hence, GRBs are stellar phenomena and their progenitors are stellar objects (Cheng & Lu 2001).

It is believed that during the GRB event a few shells of matter are ejected with different speed and when the fast shell catches up the slower one, they collide and emit γ-ray photons. This process is called an internal shock (see Piran 2005, for a detailed review).

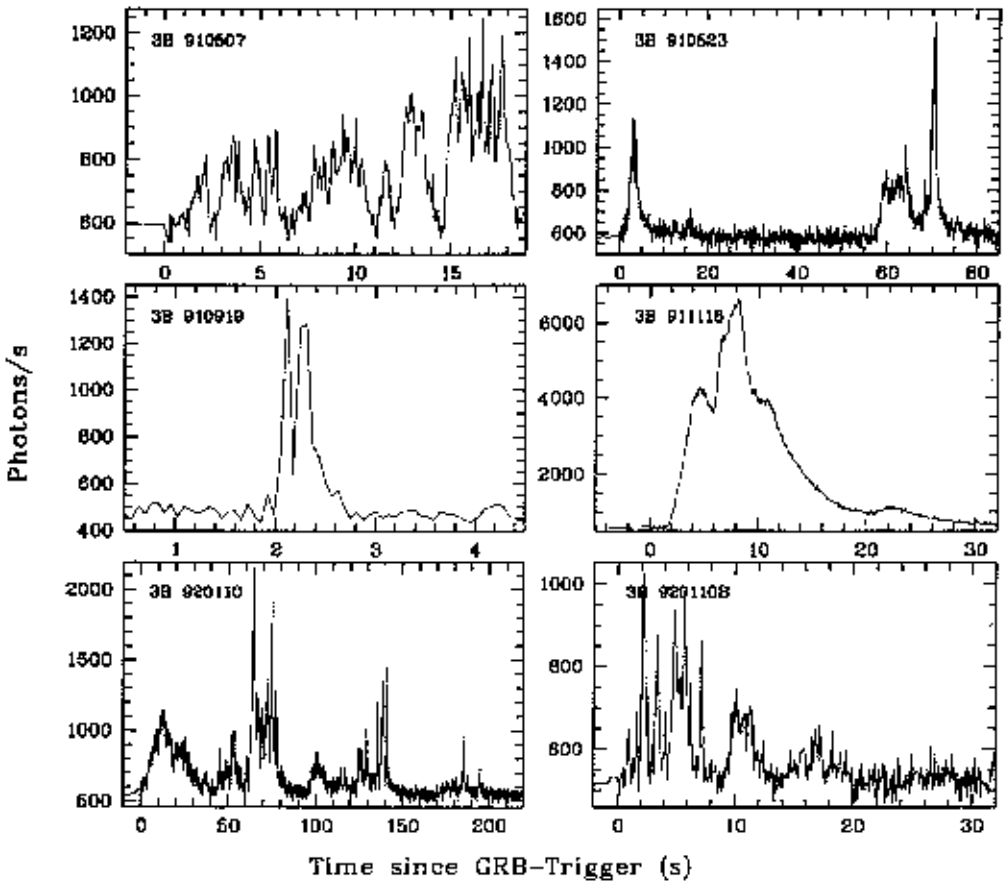

Figure 2.2: Lightcurves of some GRBs. No standard shape is apparent. GRB prompt emissions differ in terms of duration, amplitude and variability (Greiner 1999).

2.3 Progenitor

There are many proposed mechanisms for the engine of a GRB (Nemiroff 1994; Cheng & Lu 2001). However, there are two progenitors that are favoured: 1) a collapse of a massive star either being a failed supernova or a hypernova (Woosley 1993; Paczyński 1998), and 2) the merger of two compact objects such as neutron stars or black holes (Paczyński 1986). In the former case gravitational energy is released after the core collapse of the star and subsequently outer parts of the stellar eject move at ultra-relativistic velocities. In the latter scenario the merger provides the burst energy. It is believed that the collapsar model may explain properties of long/soft bursts

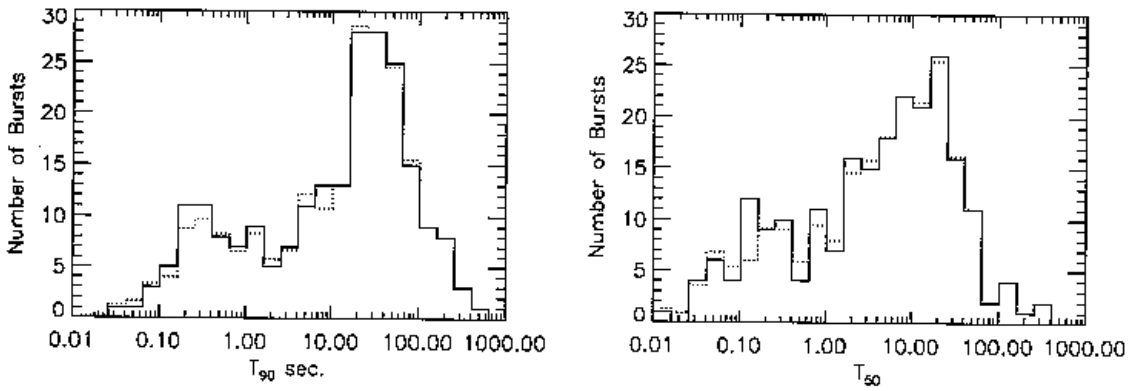

Figure 2.3: Distribution of durations of GRBs: Left (Right) — time during which counts increases from 5% to 90% (50%) above the background (Greiner 1999). A clear bimodality of duration is especially visible in the case of T_{90}.

whereas the merger model corresponds to short/hard bursts (Narayan et al. 2001).

Discoveries of GRBs associated with supernovae (SNe) were important evidence that favours the collapsar model. SN 1998bw was observed in an error box of the closest known GRB which occurred on 25 April 1998 (Galama et al. 1998). However, both GRB 980425 and SN 1998bw had a very peculiar nature, namely the isotropic energy released by the GRB was only $\sim 8 \times 10^{47}$ erg, four orders of magnitude less than a typical value and no "classical" afterglow was detected (Hjorth et al. 2004). SN 1998bw had unusually high kinetic energy and radio emission. Moreover, according to the model of redshift and luminosity distributions of GRB hosts developed by Hogg & Fruchter (1999) it was highly unlikely to find such a close GRB. Hence, it was questionable if it provided any evidence that other, more "standard" GRBs can also be claimed to be associated with supernova explosions.

More evidence for GRB–SN association was presented by Hjorth et al. (2003b) and Stanek et al. (2003) for GRB 030329 and SN 2003dh. During the early epoch of the afterglow evolution the spectrum was a power-law typical for this event. A few weeks later when the afterglow component had faded, observations revealed a supernova-like bump in the optical lightcurves as well as Fe-group lines and other spectral signatures similar to type Ic SNe[2]. A type Ic SN is believed to be the collapse of a very massive Wolf-Rayet star ($M > 20 M_{\odot}$) after the phase of extensive mass loss. It could also be a star

[2]Type Ic SNe are defined as ones with no hydrogen, helium and silicon absorption lines, see Figure 2.4 (Wheeler & Harkness 1990; Filippenko 1997)

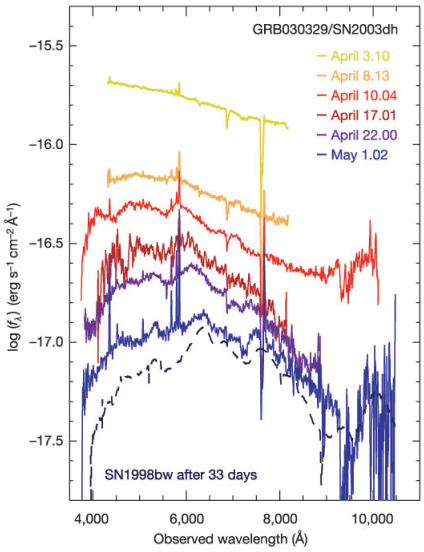

Figure 2.4: Spectrum of GRB 030329 (solid lines) and SN 1998bw (dashed line) for comparison. The early-time afterglow spectrum was a typical power-law but later a supernova-like bump dominated (Hjorth et al. 2003b).

in a binary system that looses hydrogen due to Roche lobe overflow (Nomoto et al. 1994).

The fact that a sample of GRBs associated with SNe consists only a few events (e.g. Sollerman et al. 2005; Stanek et al. 2006) can be explained by a high mean redshift of GRBs equal ~ 1 in the pre-*Swift* era and ~ 2.8 for the *Swift* sample (Jakobsson et al. 2006). It implies that a SN peak would be fainter that $R > 23$ mag which is below the detectability threshold of most ground-based telescopes (Stanek et al. 2003).

Discussion of other indirect evidences that GRBs are associated with the collapse of massive stars can be found in Section 3.3.

2.4 Afterglow

GRBs are followed by emission from X-ray to radio wavelengths. This is known as an afterglow. It was discovered in different wavelengths by Costa et al. (1997), van Paradijs et al. (1997) and Frail et al. (1997). The afterglow lasts from a few days to several months and fades away as a decaying power-law so the total flux can be written as:

$$f = f_0 t^{-\alpha} + f_{\rm gal} \tag{2.1}$$

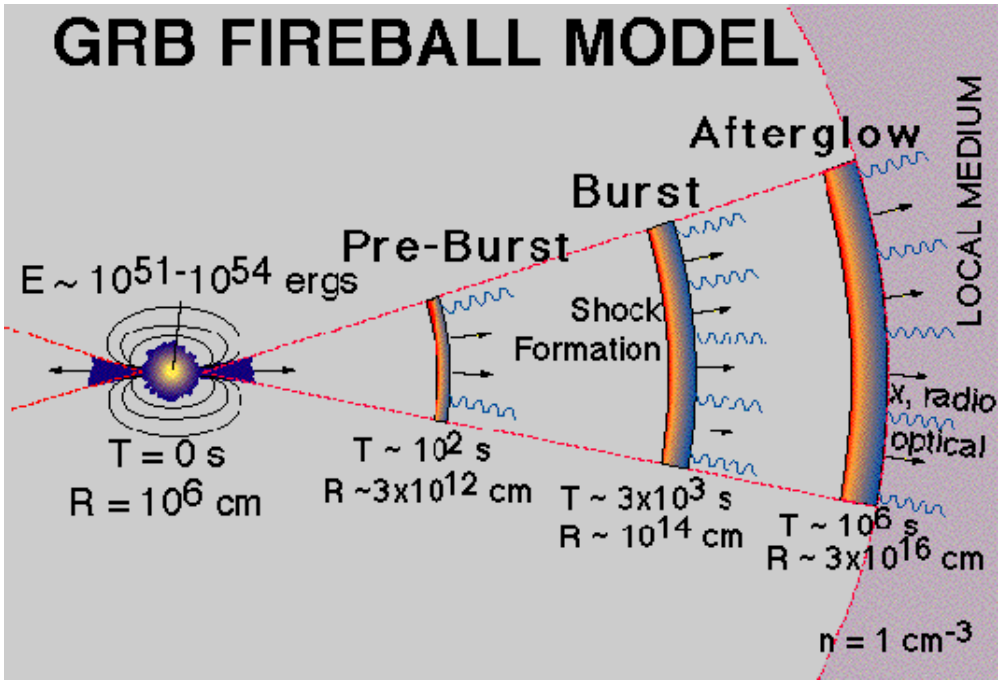

Figure 2.5: The mechanism of a GRB and its afterglow. Shock fronts are expelled from the progenitor. When the faster front catches up the slower one γ-ray photons are emitted (burst). Subsequently, the shock front collides with the surrounding medium. Synchrotron photons emitted by shocked electrons lead to the afterglow (Ghisellini 2001).

where f_0 is the initial afterglow flux extrapolated to the moment of the explosion ($t = 0$), $f_{\rm gal}$ is the flux of an underlying host galaxy and $\alpha > 0$ is a power-law index (e.g. see Castro-Tirado et al. 1999; Christensen et al. 2004a).

In addition the study of afterglows provides insight into the burst physics and conditions of the surrounding area.

The material ejected during a GRB event sweeps through the interstellar medium (ISM) and collides with gas and dust. The electrons in the medium are accelerated having a power-law distribution of energies $N(E) \propto E^{-p}$, where p is an electron index equal $\sim 2.1 - 2.9$ (Yost et al. 2003). These electrons then emit synchrotron radiation. This is believed to be the mechanism of the GRB afterglow (Piran 1999) and is called an external shock. In Figure 2.5 the right most color strip corresponds to the collision of a shock front with the ISM when afterglow photons are produced, whereas the two former strips indicate burst of γ-rays (the internal shock, see Section 2.2) .

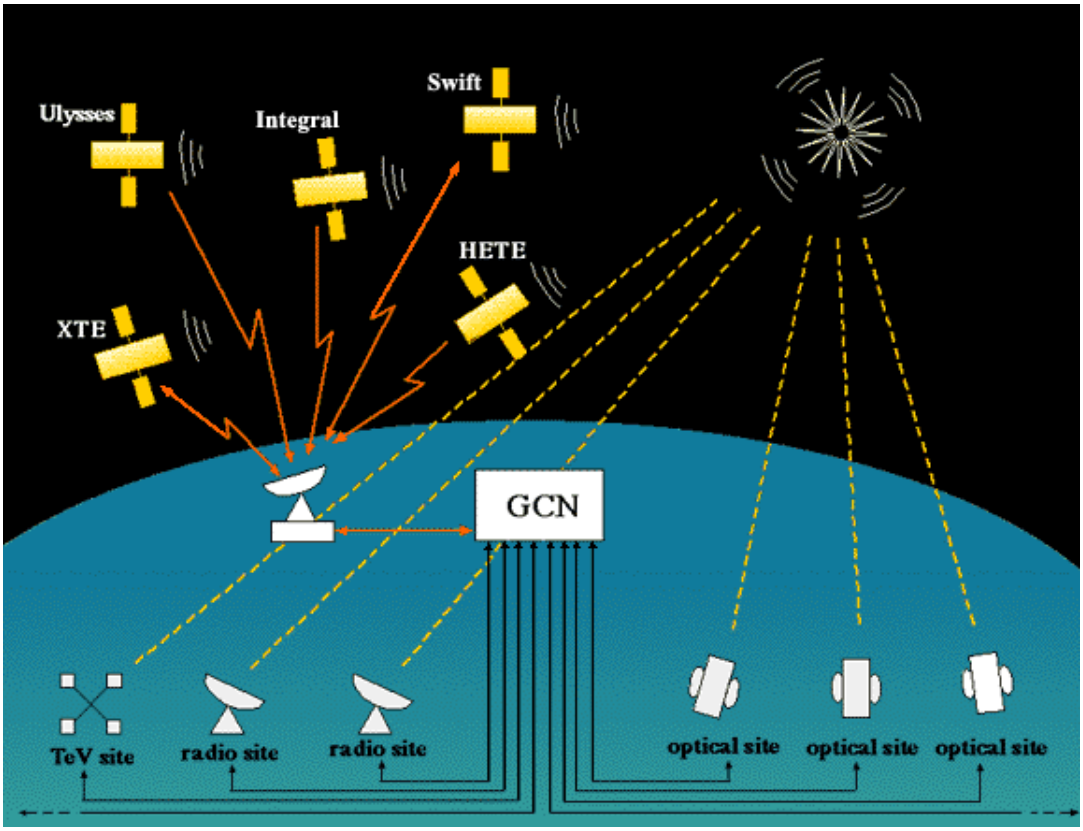

Figure 2.6: The GCN connection network. Once a GRB is detected by one of the γ-ray satellite, rapid follow-up is conducted from the ground at a variety of wavelengths. Source: `http://lheawww.gsfc.nasa.gov/docs/gamcosray/legr/bacodine/GCN.gif`

One popular model of the afterglow emission is the so-called "fireball model" (Cavallo & Rees 1978; Goodman 1986; Paczyński 1986; Rees & Meszaros 1992; Meszaros & Rees 1997). It assumes that an ultra-relativistic blast of a radiation-electron-positron plasma sweeps through the surrounding medium. The blast wave is assumed to be adiabatic and very hot. This results in the production of electron-positron pairs. After the temperature drops below the rest mass of an electron (0.5 MeV) the annihilation is faster than the creation and additional photons are emitted.

Modeling of multi-band lightcurves of the afterglows provides a very important tool for interpreting the mechanism of GRB (e.g. Berger et al. 2001a; Castro Cerón et al. 2002). For example, it can help to distinguish between the hypernova and the binary models. In the former case the burst goes

through the medium which is a result of stellar mass-loss with a density profile vs. distance from the GRB progenitor varying as $\rho \propto r^{-2}$. In the case of the binary model the burst occurs in a uniform ISM. These two models imply different evolution of the afterglow at different wavelengths and it can be directly compared with observational data.

The simple picture of the afterglow power-law decay (equation 2.1) is not actually fulfilled in many cases because breaks in the lightcurves may occur. These breaks may result either from density profiles of the surrounding medium that can cause the decelerating of the outflow or from the beaming. If they occur in each wavelength they are called achromatic breaks. Otherwise they are chromatic breaks. If the break is in the form of a steepening of decay rate (α changes to a higher value) it implies a homogeneous medium. Shallowing implies a wind-like medium (Sari et al. 1998). Chevalier & Li (1999) found that some of GRBs are consistent with a wind (980326, 980425, 980519) and some with the uniform model (970228, 970508, 990123).

The detailed modeling of the afterglow lightcurves provides some evidences for collimated rather than spherical outflows (e.g. Castro Cerón et al. 2002). The presence of a collimated jet was proven by both the achromatic breaks in the lightcurves of afterglows and by their fast decay rates (Sari et al. 1999; Panaitescu & Kumar 2002). Jet and spherical expansions can be distinguished because when the relativistic outflow decelerates we observe a larger fraction of the jet due to a decrease of a Lorenz contraction, which limits the observable surface of the cone. At some point this mechanism is stopped for the jet outflow when the observable cone is larger than the jet cone (Ghisellini 2001; Piran 2001). Granot (2003) claimed that the reported high degree of polarization (80%) of prompt emission of GRB 021206 implies synchrotron emission and the presence of strong, ordered magnetic field which was involved in the jet formation.

2.5 GRB Networks

Afterglows are possible to observe from the ground in different wavelengths because information about a new GRB is distributed quickly among astronomers via the Gamma ray bursts Coordinates Network (GCN)[3]. Figure 2.6 shows schematically how the GCN works. After the initial detection of a GRB, X-ray telescopes try to refine the error box to the accuracy of half to several arcminutes (Hogg & Fruchter 1999). Then optical to radio

[3] `http://lheawww.gsfc.nasa.gov/docs/gamcosray/legr/bacodine/gcn_main.html`

observations are carried out in order to cover this error box and detect an afterglow.

GRB afterglows are observed within Target-of-Opportunity (ToO) programs. ToO time allows observers to postpone the scheduled observations in favor of transient and unpredictable objects such as GRBs, SNe, novae, comets, X-ray bursters, soft gamma repeaters, etc. Many telescopes from X-ray to radio operate ToO observations what allows rapid detections of afterglows and reasonable temporal coverage of the lightcurves.

Chapter 3

GRB Host Galaxies

3.1 Short-Wavelength Observations

Long after a GRB event, when the afterglow emission has become negligible, the GRB host galaxy can be observed. The first interpretation of a constant extended source as the host galaxy and analysis of its properties was proposed by van Paradijs et al. (1997); Sahu et al. (1997). Alternatively, one can detect the host indirectly, by fitting a power-law to the afterglow lightcurve and a determining the flux of the galaxy using equation (2.1).

Le Floc'h et al. (2003) reported that GRB host galaxies were very blue ($R - K \lesssim 3$), even more so than nearby irregular galaxies. Moreover, they were sub-luminous ($K > 20$, $M_K \sim -22.25 = 0.08 M_\star$), which implied low stellar masses. It could indicate that they were young galaxies undergoing the first episode of star-formation. Similar results were reported by Savaglio et al. (2006), using a sample of 32 hosts, most of which had a stellar mass $< 10^{10} M_\odot$, age < 400 Myr and high specific SFR, and also by Christensen et al. (2004a), with 10 young starburst hosts, with low extinction and high specific SFRs compared to field galaxies. This is shown on Figure 3.1, where GRBs are clearly more star-forming than the average field galaxy. Recently, Fruchter et al. (2006) claimed that their sample of 42 GRB hosts were irregular blue galaxies, whereas only one GRB host (030115) to date can be classified as an Extreme Red Object, with $R - K = 5$ (Levan et al. 2006). However, this host was not detected in submm (see Table 4.1 and Smith et al. 2005). Thus, GRB hosts seem to be similar to the population of faint blue star-forming galaxies at high redshift, but not to the population of dusty submm highly star-forming galaxies which are brighter in K-band and redder.

Spectroscopical observations of hosts also provide some indication of the

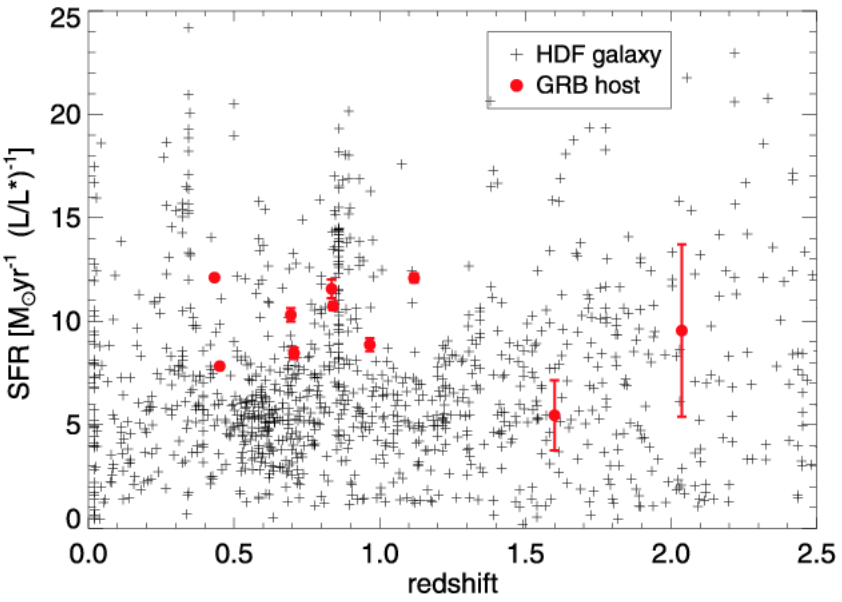

Figure 3.1: The specific SFR per unit luminosity of GRB hosts (filled circles) and Hubble Deep Field (HDF) galaxies (crosses). GRB hosts are on average more star-forming than the HDF sample (Christensen et al. 2004a).

massive star-formation by high ratios of [Ne III] and [O II] lines, which require photoionization by massive stars (Djorgovski et al. 1998, 2001; Sollerman et al. 2005).

These findings can be explained by theoretical models. MacFadyen & Woosley (1999) predicted that the formation of massive rotating helium stars — progenitors of GRBs — was favored in low metallicity regions. This is because, in the case of high metallicity, strong stellar winds induce strong mass and angular momentum losses, which hamper the formation of GRBs. Hence, dwarf and subluminous galaxies would be preferred as hosts (Le Floc'h et al. 2003), since they usually have lower metal content. Metal-poor environments of GRB hosts are also preferred by their enhanced Lyα emission (Fynbo et al. 2003; Jakobsson et al. 2005), low oxygen abundances (Stanek et al. 2006), characteristics of emission lines (Vreeswijk et al. 2001; Bloom et al. 2003; Gorosabel et al. 2005), SMC[1]-type of extinction (Kann et al. 2006), value of dust-to-gas ratios similar to, or even lower than, that of the SMC (Hjorth et al. 2003a; Stratta et al. 2004; Kann et al. 2006) and somewhat small sizes and irregular morphologies (Fruchter et al. 2006). Savaglio

[1]Small Magellanic Cloud

et al. (2003, 2006) found that metallicity of GRB hosts is usually less than $0.6Z_{\odot}$, which is typical for starburst galaxies.

A preference for low metallicity can explain the lack of detections in submm (see Section 3.2 and Chapter 4) and the nondetection of GRBs hosted by a galaxies similar to red highly-starforming galaxies (such as Arp220), because such objects are usually metal-rich (Fruchter et al. 2006).

Optical searches have confirmed the low extinction of GRB hosts (e.g. Christensen et al. 2004a; Chen et al. 2006b) and that the extinction may be correlated with submm SFR (Kann et al. 2006). This is expected as higher SFR implies higher dust content. Savaglio et al. (2003) claimed, that in spite of low reddening, there might be significant amount of dust in GRB hosts, as indicated by absorption lines. They proposed that the dust caused rather gray absorption, which is possible if there is a deficiency of small grains, which may have been destroyed by the GRB event (Fruchter et al. 2001).

Generally, optical SFR indicators give 1–2 orders of magnitude smaller values than submm and radio (see Chapter 5 and also Berger et al. 2003), which clearly indicates that the majority of star-formation activity is hidden by dust. However, the radio/submm-detected hosts form a very limited sample, whereas the other hosts show no detectable long-wavelength emission, thus indicating moderate or low SFR $\lesssim 100 M_{\odot}$/yr (Berger et al. 2003). Moreover, Watson et al. (2004) placed firm upper limits on the total SFRs of three hosts, with SFR $\lesssim 2.8$, $\lesssim 200$ and $\lesssim 150 M_{\odot}$/yr, using an unobscured X-ray indicator which tracks high mass X-ray binaries. In summary, GRB hosts (as a whole) do not seem to be highly star-forming, but rather have high specific SFRs.

Mid-infrared observations of GRB hosts were carried out recently by Le Floc'h et al. (2006) with 4.5, 8.0 and 24 μm *Spitzer* filters. From a sample of 16 galaxies, the detection level was 20%. It confirmed the picture of hosts as moderately star-forming dwarf galaxies. Using the same data, Castro Cerón et al. (2006) estimated stellar masses (median $5.6 \times 10^9 M_{\odot}$) and SFRs (in a range $0.5 - 428 M_{\odot}$/yr), suggesting young and low stellar populations and very high specific SFRs of the hosts.

The optical to mid-infrared fluxes of the GRB hosts discussed in this thesis are reported in Table 6.1.

3.2 Long-Wavelength Observations

If GRBs were tracers of star-formation activity (see Section 3.5) they would be expected to be hosted by galaxies with high submm luminosity. In particular, 10% of hosts would be expected to have fluxes greater than 5 mJy

at 850 μm (Ramirez-Ruiz et al. 2002). However this has turned out to be incorrect. Tanvir et al. (2004) reported that only few hosts were detected in submm (000210, 000418, 010222), accompanied by a few tens of non-detections (see Chapter 4). Only a few hosts were (weakly) detected at significant levels in radio wavelengths: GRB 980703 (the first radio host detection; Berger et al. 2001b), GRB 000418 (Berger et al. 2003) and GRB 010222 (Berger et al. 2003; Frail et al. 2002). In addition, several hosts were detected at $\gtrsim 2\sigma$ level (Berger et al. 2003). Summarizing, both radio and submm observations only revealed a small number of hosts with SFRs of the order of a few$\times 100 M_{\odot}$/yr, which possibly form the bright-end of the host sample.

Nevertheless, this lack of detections is not inconsistent with the hypothesis that GRBs are star-formation tracers. As outlined in Section 3.1, GRB hosts are likely to be subluminous dwarf galaxies and hence have small overall SFRs (low submm fluxes) as opposed to specific SFRs. Tanvir et al. (2004) also claimed, that the distribution of submm fluxes of GRB hosts was consistent with the evolutionary model of a submm galaxy population described by Blain et al. (1999a,c); Ramirez-Ruiz et al. (2002). Trentham et al. (2002) claimed that these non-detections agreed with a hypothesis that much of the star-formation in the Universe occurred in galaxies with submm fluxes below 4 mJy at 850 μm, and thus rare detectable by SCUBA. GRB hosts may be members of this sample.

It is interesting to note, that there were no dark GRB hosts detected in submm (Barnard et al. 2003) although they were believed to show no optical afterglow due to large amount of dust in the hosts.

Submm-mm observations of GRB 010222 yielded a steep spectral slope equal to $\beta = 1.78 \pm 0.25$, which was likely to be caused by dust thermal emission dominating in this wavelength range, as reported by Frail et al. (2002). They also claimed that the significant submm emission can not be explained by the heating due to the GRB event itself and must be an indicator of a starburst within the galaxy.

A similar conclusion was drawn from radio observations of the GRB 980703 host — the emission was powered by the starburst, not by the Active Galactic Nucleus (AGN) — as Berger et al. (2001b) detected no variability in the radio flux over 650 days. Moreover, high-ionization lines like [O III] have not been found, or were weak, in the host spectra (Djorgovski et al. 1998; Berger et al. 2001b). Based on a luminosity function of GRBs, Fenimore et al. (1993) also rejected (at 90% confidence) a hypothesis that AGNs resided in GRB hosts. The presence of AGNs in GRB hosts will ultimately be confirmed or ruled out by presently scheduled X-ray observations.

The far-infrared to radio fluxes of the GRB hosts discussed in this thesis

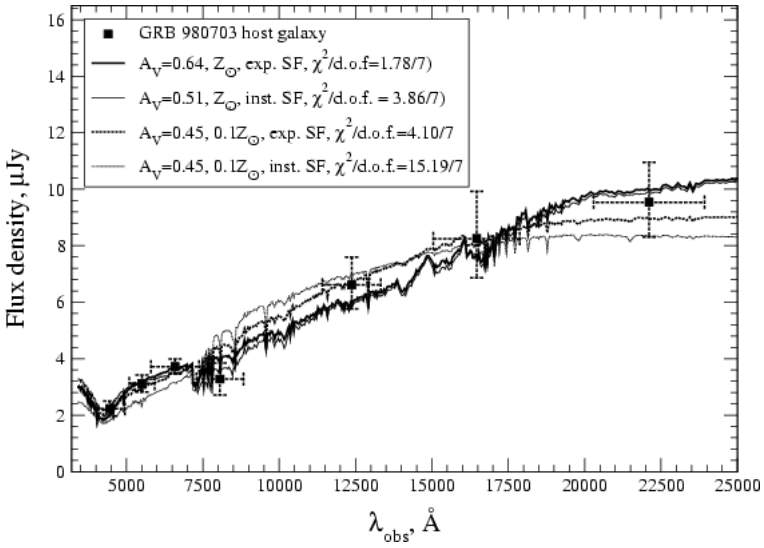

Figure 3.2: The fits to an optical part of GRB 980703 SED (Sokolov et al. 2001). Starburst templates are the most consistent with the data.

are reported in Table 5.1.

3.3 Implication for Progenitor Physics

Investigations of GRB hosts are very important to understanding the nature of GRBs. If the collapsar model is correct, then GRBs should occur in galaxies with high SFRs or at least with high specific SFRs per unit stellar mass, because new stars are born in such environments, especially the massive, short-lived stars — progenitors of GRBs (see Hjorth et al. 2004, for a review). In contrast, massive stars in old environments have already finished their lives. Indeed, there is some evidence to support the idea that GRB hosts are star-forming galaxies. For example, Berger et al. (2001b, 2003); Frail et al. (2002); Tanvir et al. (2004) reported that some GRB hosts are starburst galaxies with SFRs of several hundred solar masses per year (see also Chapter 7).

Before the discovery of the GRB–SN association (see Section 2.3), only indirect evidence was available for GRBs being collapses of massive stars, namely that they occur in star-forming regions. For example, Holland & Hjorth (1999) investigated the Hubble Space Telescope (HST) image of the surroundings of GRB 990123 and found that it occurred in an irregular galaxy, consisting of three knots with sizes comparable to the star-forming

and HII regions in the local Universe, as well as having luminosities and flat spectra consistent with it being star-forming. Similarly, Bloom et al. (1998, 1999a); Galama et al. (1998); Kulkarni et al. (1998b); Paczyński (1998); Castro-Tirado & Gorosabel (1999); Fruchter et al. (1999a,b); Hjorth et al. (1999, 2000, 2002); Fynbo et al. (2000); Holland (2001); Prochaska et al. (2004) claimed that GRBs resided in star-forming regions. In the case of GRB 980425 the region within 100 pc from the GRB contained three stars with blue colors consistent with being massive main-sequence stars (Holland 2001).

A more systematic approach to this issue was taken by Bloom et al. (2002). They investigated a sample of 20 long duration GRBs and measured their offsets from the centers of the hosts, getting a small median value equal to $0.17''$ (1.3 kpc). Moreover, this value was equal to 0.98 of the half-radii of the hosts, suggesting that GRBs traced the UV-emitting regions. Both findings supported a connection of GRBs with star-formation and, in turn, with the collapsing massive star model. This is because the lifetime of a massive star is $\lesssim 10^7$ yr, whereas a binary system needs $\sim (2-10) \times 10^7$ yr to coalescence, giving it enough time to escape from its place of birth. The observed distribution was also in agreement with a predicted distribution of collapsars rather than merging binaries (see also Bloom et al. 1999b; Bulik et al. 1999a,b, where offsets as high as 100 kpc or even 1 Mpc were predicted for the binary model).

Recently, Fruchter et al. (2006) confirmed these findings on 42 GRB hosts using a better technique based on a localization of GRBs with respect to the brightness of pixels in the hosts. They found that GRBs not only trace UV light but the brightest UV parts of galaxies. It confirmed that their progenitors are extremely massive stars, which usually reside in so-called stellar associations giving rise to the brightest UV emission. The luminosity function of GRB hosts appeared to be similar to the Lyman-Break Galaxies, further indicating that they trace UV light (Jakobsson et al. 2005).

Bloom et al. (2002) did not find any GRBs residing in an elliptical (old) galaxy, which would be expected for merging binaries. Similarly, Conselice et al. (2005) claimed that GRB host light profiles were slightly more consistent with spiral (exponential disk) than elliptical (de Vaucouleurs) profiles. However, in some cases they found some indication of a late-type morphology (with a nuclear starburst), such as high concentration.

Spectral properties of afterglows provide an additional clue in favour of the collapsar model. Metal lines in X-ray afterglows indicate enrichment from explosions of massive stars (Piro et al. 1999, 2000; Antonelli et al. 2000; Amati et al. 2000; Reeves et al. 2003; Butler et al. 2003; Watson et al. 2003; Chen et al. 2006a). Moreover, multiple velocity components seen in optical

afterglows resemble the shell structure around a massive star (Schaefer et al. 2003; Mirabal et al. 2003). The presence of strong emission lines ([O II], [O III], Lyα, Balmer and Pashen series, [N III]) indicates a star-formation activity (Bloom et al. 1998; Kulkarni et al. 1998a; Pian et al. 1998; Fynbo et al. 2003; Hjorth et al. 2003b; Christensen et al. 2004b).

Another indirect evidence for GRBs being associated with star-forming regions came from an attempt to model the redshift and luminosity distributions of GRB hosts, made by Hogg & Fruchter (1999). They investigated three models in which a GRB rate was proportional to the SFR (consistent with the collapsar model), to the total integrated stellar density (consistent with the merger model) or was constant at any redshift. They found that the first model was slightly favored, whereas the second was most strongly disfavored by the data (the likelihoods' ratio was 1.00 : 0.12 : 0.57). Proportionality between GRB rate and SFR was also claimed by Totani (1997); Mao & Mo (1998); Wijers et al. (1998); Kommers et al. (2000)

Numerical simulations of large-scale formation also showed that GRB hosts are actively star-forming, low-mass, young galaxies (Courty et al. 2004).

Finally, Sollerman et al. (2005) were able to estimate the mass of the progenitor, equal to $30 \pm 5 M_{\odot}$, by analysing the colors and the spectrum of the GRB 980425 host, determining the age of the starburst and thus the minimal mass of the progenitor. The value agrees with the collapsar progenitor hypothesis (see Section 2.3).

3.4 Spectral Energy Distributions

Some previous attempts to analyse the SEDs of GRB hosts have already been made, but not at the same level of wavelength-coverage and self-consistency as presented in this work. Sokolov et al. (2001); Gorosabel et al. (2003a,b, 2005); Christensen et al. (2004a, 2005) constructed models of the optical parts of the SEDs, which fitted the photometric data of GRB hosts. An example is shown in Figure 3.2. They were able to constrain several characteristics of the hosts, such as the ages, masses of the bursts, metallicities and extinction. They concluded that the best fits were obtained for starburst templates.

Recently Priddey et al. (2006) tried to constrain the FIR luminosity of GRB 030115 host using an estimation from optical extinction. Deep mm and submm upper limits allowed them to put a lower limit on the dust temperature, equal to 50 K, as shown in Figure 3.3.

As noted above, Castro Cerón et al. (2006) fitted templates of starburst and quiescent galaxies to the broad-band data of GRB hosts and derived their SFRs, stellar and dust masses. That work was based on the SED

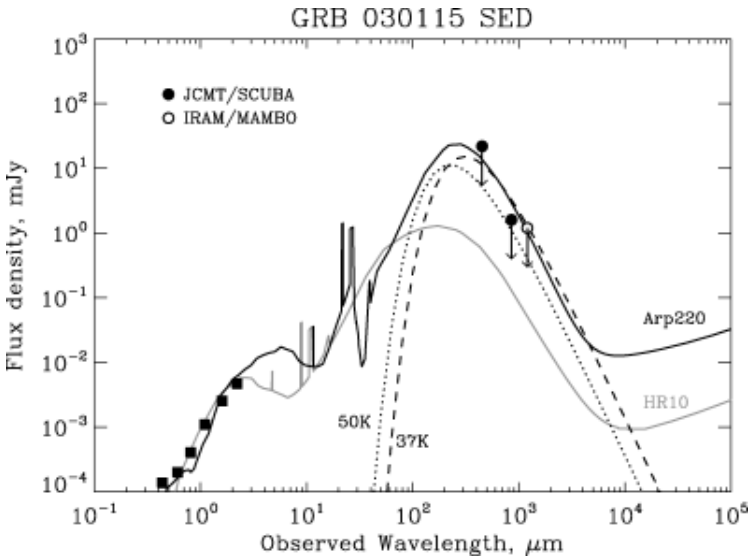

Figure 3.3: The SED of GRB 030115. Data (squares and circles) and templates (lines) are shown. The far-infrared gray-body spectra are constructed with luminosities derived from optical extinction. In order to be consistent with the upper limits, the temperature of dust must be larger than 50 K (Priddey et al. 2006).

fitting formalism developed in this thesis.

Summarizing, a multi-wavelength SED approach to the host observations has a great capability in constraining the galaxy properties, but it seems that not all the data, especially at longer wavelengths, have yet been thoroughly analysed.

3.5 Star Formation History

One of the issues in the understanding of the evolution of the Universe, is its Star Formation History. It is quantitatively described by so-called Madau diagram (Madau et al. 1996, 1998; Lilly et al. 1995), giving specific SFR (per unit volume) as a function of redshift (Figure 3.4). There are many possible ways to estimate SFRs (see caption of Figure 3.4 and Kennicutt 1998, for a review). However, all of them rely on the choice of the galaxy population on which they are applied. This introduces selection effects, such as favoring less-dusty environments, flux limitation and color selection, etc.

These selections effects do not apply in the case of GRBs because γ-rays are not extinguished by dust and they are bright enough to be seen from long

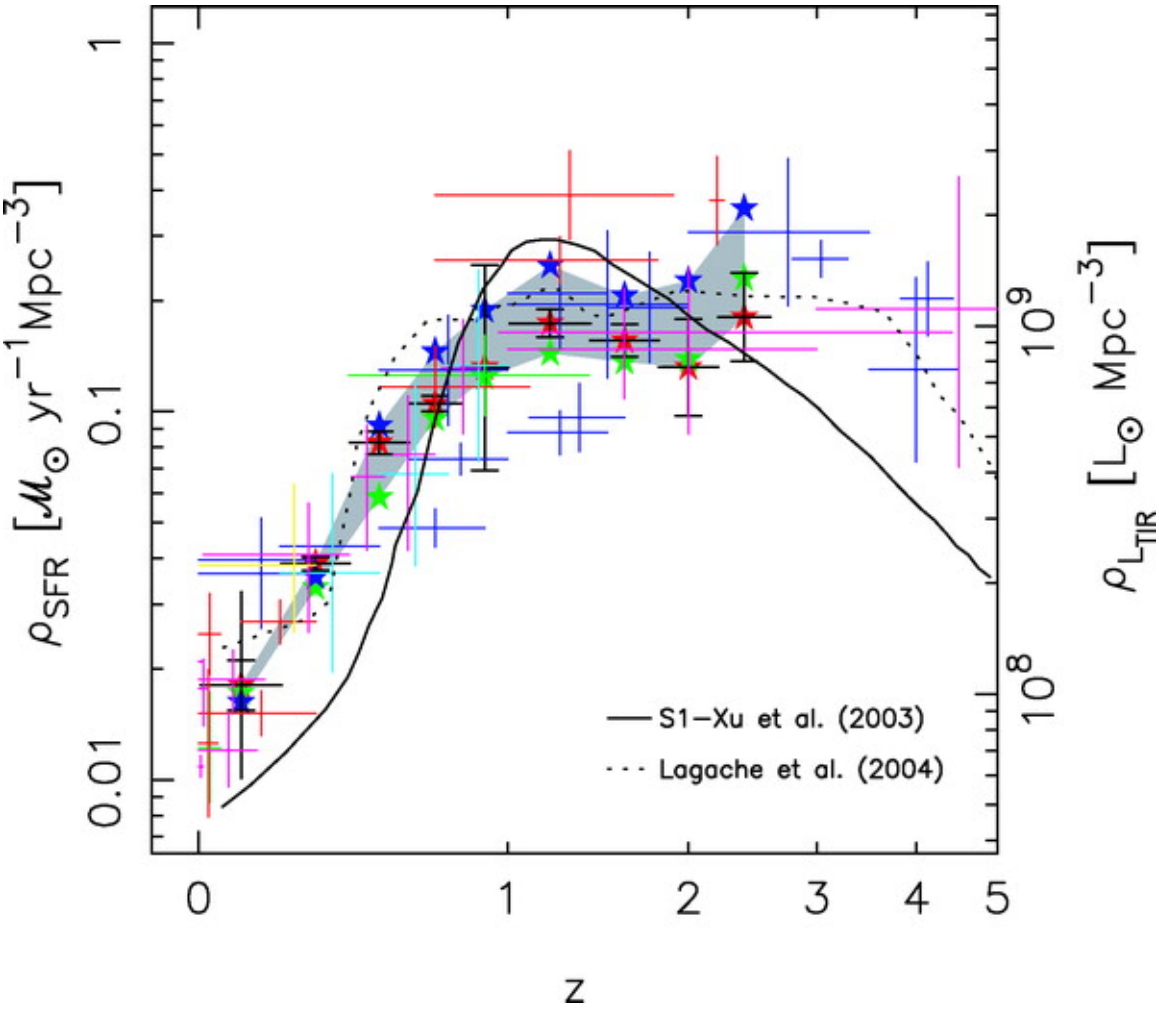

Figure 3.4: The Madau diagram — the SFR density as a function of redshift. Different SFR indicators are shown with different colors: $H\alpha$ and $H\beta$ (red), [O II] (green), UV continuum (blue), MIR emission (cyan), submm and radio emission (red), X-ray emission (yellow). Two theoretical models are given for comparison (Pérez-González et al. 2005).

distances, even up to $z = 15 - 20$ as predicted by Lamb & Reichart (2000). If GRBs are connected with the deaths of massive stars, then they occur shortly after the starburst in the host (see Section 3.3) and can therefore be an excellent probe of star-formation (Totani 1997; Wijers et al. 1998; Mirabel et al. 2000; Blain & Natarajan 2000). Hence, the properties and SFRs of their hosts should be investigated carefully. This study requires a

significant sample of observed at multiple wavelengths GRB hosts with a good redshift coverage. The redshift determination of GRB hosts is easier than that of other distant galaxies, because although both can be too faint to perform spectroscopy, the GRB afterglow can be sufficiently bright (Le Floc'h et al. 2003). Finally, if the relation between the star-formation and the GRB rate is established, it can be used regardless of whether the host has been detected or not.

There are some possible biases and problems associated with using GRBs as tracers of star-formation. For example, Jakobsson et al. (2005); Stanek et al. (2006); Wolf & Podsiadlowski (2006) claimed that nearby GRBs are connected with the low-metallicity star-formation, rather than the total star-formation. However, this should not be a problem at high redshift ($z \gtrsim 2$), because the average metal content was lower at that time (Conselice et al. 2005; Wolf & Podsiadlowski 2006).

Moreover, a GRB host population is different from highly-starforming galaxies (Le Floc'h et al. 2003). This could indicate that some star-formation activity is missed in GRB host studies. Additionally, understanding the star-formation activity of GRB hosts is difficult, because the known sample may be biased towards dust-free objects, as the redshift determination is mostly achieved by spectroscopy of bright optical afterglows.

Chapter 4

SCUBA Data Reduction

4.1 Introduction

Recently, several detections of GRB host galaxies were achieved at submillimetre (submm) wavelength (Tanvir et al. 2004) with the Submillimetre Common-User Bolometer Array (SCUBA, Holland et al. 1999)[1] mounted at the James Clerk Maxwell Telescope (JCMT), Mauna Kea, Hawaii. Namely, hosts of GRB 000210, GRB 000418 and GRB 010222 were detected. However, they were weak detections at the significance level of 4σ, 3.5σ and 7σ, respectively. Additionally, the host of GRB 980613 were detected at a marginal 2σ level. Hence, I re-reduced these data to revise the reliance of these detections and confirm the remaining non-detections.

4.2 Telescope and Detector

The JCMT is located at a longitude of $155^o28'47''$W, a latitude of $19^o49'33''$ and at an altitude of 4092 m, which is a perfect site in terms of low atmospheric influence (see Section 4.4.2). The telescope is shown on Figure 4.1. The primary mirror has the diameter of 15 m.

The SCUBA is a submm receiver consisting of two arrays working at $850\,\mu$m (37 pixels) and $450\,\mu$m (91 pixels) — at two of several atmospheric windows in the submm domain (Figure 4.2). The pixel layout and the optics are shown on Figure 4.3. The arrays have a field of view of 2.3 arcmin. The primary beam size (the diffraction limit of the resolution) is 14 and 7.5 arcsec for $850\,\mu$m and $450\,\mu$m, respectively. Both arrays can be used simultaneously by means of a dichroic beamsplitter. There are two mapping modes available:

[1] `http://www.jach.hawaii.edu/JCMT/continuum/`

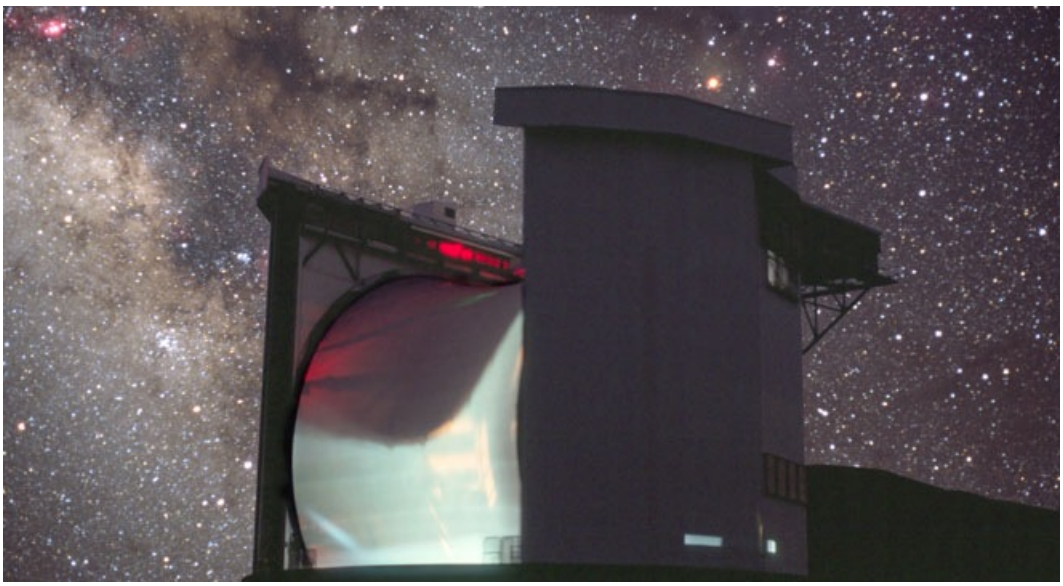

Figure 4.1: Night view of James Clerk Maxwell Telescope. Source: `http://www.jach.hawaii.edu/JCMT/`

jiggle and scan. The telescope is "jiggling" around the source in the former case and scanning the sky in the latter. In the photometry mode only a central pixel is used. The SCUBA is cooled down to 100 mK to provide small thermal noise and good sensitivity.

At the time of writing SCUBA has finished its operating period and is going to be replaced by SCUBA-2[2] at the beginning of 2007.

4.3 Data

I downloaded the raw data from the SCUBA archive[3]. They were photometric observations of GRB host galaxies obtained in a photometry (`PHOTOM`) mode using the central pixel of SCUBA arrays. This mode was used because of its higher efficiency compared to mapping jiggle mode (Jenness et al. 2002), which is very important for faint sources such as GRB hosts. Observations were made simultaneously in 850 μm and 450 μm filters. The list of reduced sources is presented in Table 4.1.

[2] `http://www.roe.ac.uk/ukatc/projects/scubatwo/`
[3] `http://cadcwww.hia.nrc.ca/jcmt/`

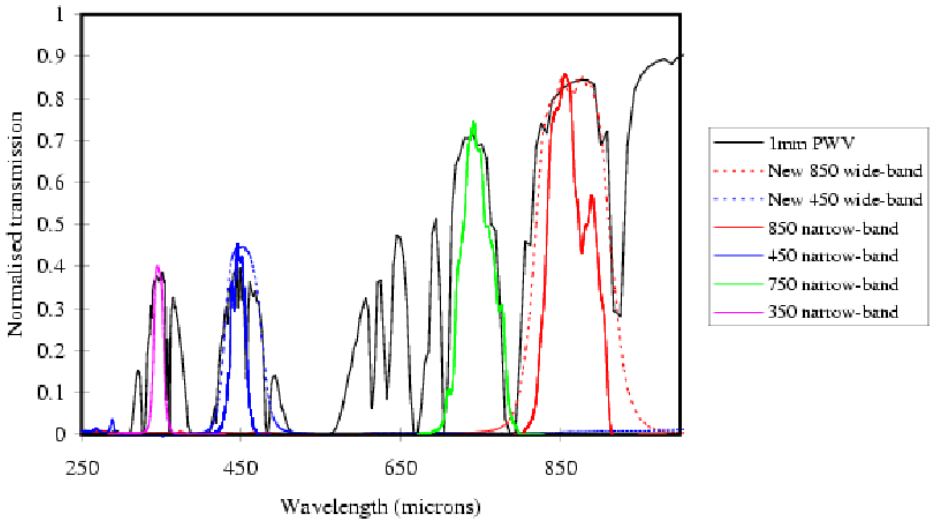

Figure 4.2: Atmospheric opacity (black) with profiles of some of the SCUBA filters (Holland et al. 1999).

4.4 Process of Reduction

The reduction was done automatically using the recipe `SCUBA_STD_PHOTOM` working in the `ORAC-DR`[4] environment (Economou et al. 1999; Jenness & Economou 1999). It performs flatfielding, extinction correction, clipping, sky noise removal and flux calibration (Jenness & Lightfoot 1998; Jenness et al. 2002).

4.4.1 Flatfielding

The different response of each bolometer is removed by division of a science image by a flatfield which is obtained by a scan-mapping of a point-like source e.g. Mars or Uranus. The flatfield remains constant with time and does not need to be re-measured every night. This is more important in the mapping mode where all pixels are used to detect the signal from the source. However, it is also performed in case of the photometry in which only the central pixel points at the source. This is because other pixels are used for a sky noise subtraction (Section 4.4.2) and because some field curvature is present at the focal plane (Holland et al. 1999).

[4]Observatory Reduction and Acquisition Control–Data Reduction pipeline

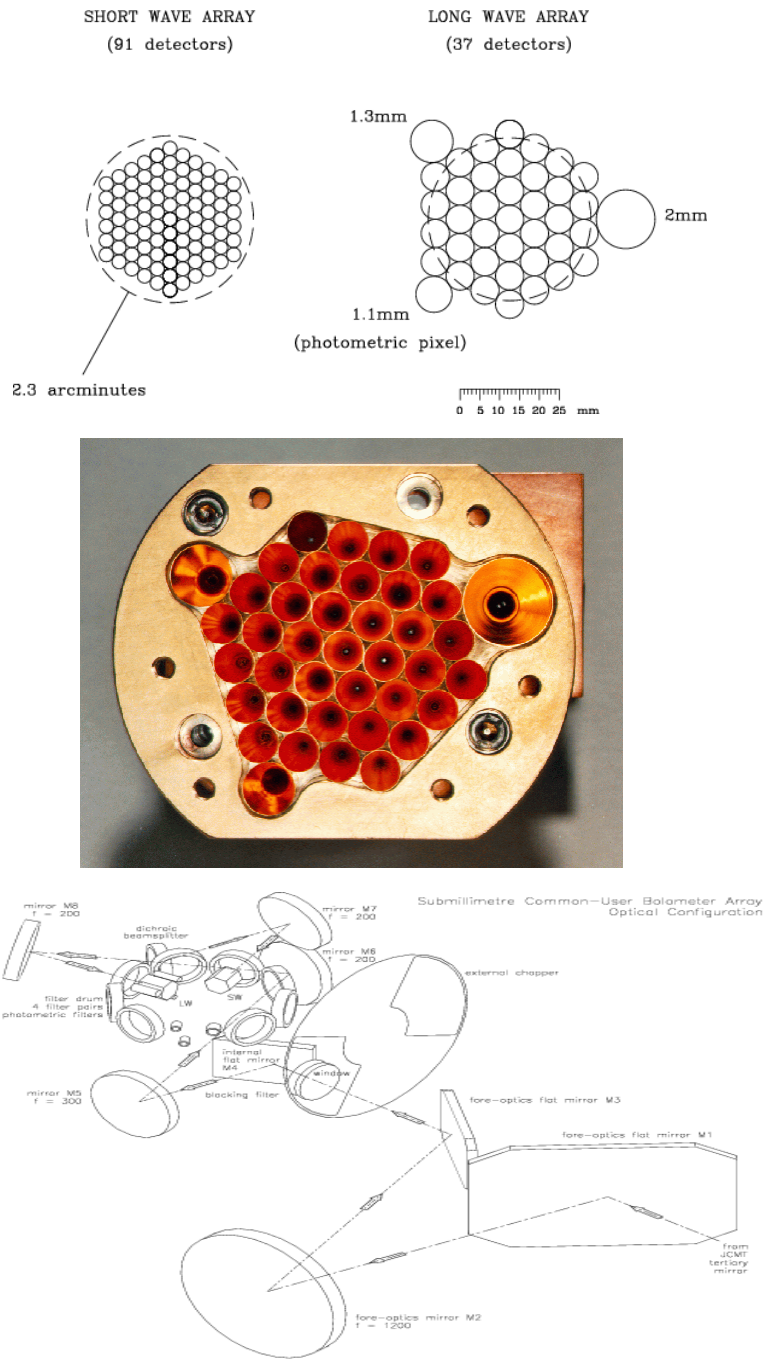

Figure 4.3: The pixel layout (top), the view of the long-wavelength array with a set of feed horns (middle) and the SCUBA optics (bottom) (Holland et al. 1999).

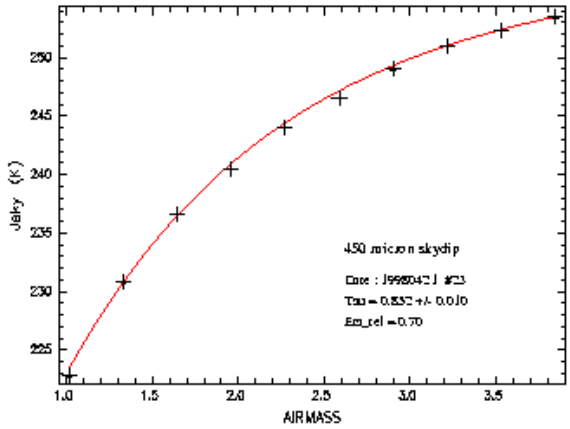

Figure 4.4: The Skydip: brightness of the sky at different elevations/airmasses. These observations allow to measure the opacity of the sky τ (Holland et al. 1999).

4.4.2 Extinction Correction

Since atmospheric attenuation in submm wavelengths is strong and varying in time, an extinction correction must be performed carefully. There are three ways to do it: 1) Several times per night so-called skydip observations are performed. They are pointings at the blank sky at different elevations with a comparison of a hot load and a cold load present in the detector, both with known temperature. This allows us to calculate the sky temperature and thus the zenith opacity τ (see Figure 4.4). 2) The JCMT-Water-Vapor-Monitor measures the opacity of the sky every 6 seconds simultaneously with target observations almost at the same direction as the main beam. 3) The Caltech Submillimeter Observatory (CSO) measures τ at 1250 μm every 10 minutes which can be transformed into the opacity at 850 μm by well-established relations (Archibald et al. 2002). A polynomial is fitted to CSO data (top panel of Figure 4.5) in order to remove influence of the noise in measurement and achieve better sampling of the relation between τ and time. This is crucial because of high instrumental noise of the CSO τ-meter. The bottom panel of Figure 4.5 shows that skydips and CSO fits are consistent. The error of the opacity derived from the fit is of the order of 0.005 (Jenness et al. 2002).

4.4.3 Clipping

Obvious spikes are removed. Individual pointings which differ more than 5σ from the average are excluded. It ensures that observations are not contaminated e.g. by cosmic rays. The clipping threshold should not be lower than 3σ in order not to remove real signal.

4.4.4 Sky Noise

Thermal radiation from the sky influences strongly the target signal because it is often several order of magnitude larger, so sky noise must be removed to get data with smaller scatter. The secondary mirror is "chopping" and "nodding" slightly around the source so the sky signal off-the source is measured and subtracted from on-the source signal. Examples of raw and sky-subtracted photometric observations are shown on Figure 4.6. On the top panel there is a noisy original signal which gets much better and stable after the sky noise removal. For sources which are not detected this can lead to a negative value of the flux (see Table 4.1). It is only the sign of statistical noise and should average to zero eventually for long enough integration time (Jenness, private communication).

4.4.5 Flux Calibration

Finally, proper conversion from volts to janskys must be done. The conversion factor is derived from observations of Mars and Uranus. The factor is equal to ~ 210 Jy/V for 850 μm and ~ 260 Jy/V for 450 μm.

4.5 Applying the Reduction

I downloaded the `ORAC-DR` and executed following commands

```
source /star/etc/login
source /star/etc/cshrc

setenv ORAC_DIR /linux/opt/oracdr
setenv ORAC_CAL_ROOT $ORAC_DIR/cal
setenv ORAC_PERL5LIB $ORAC_DIR/lib/perl5
setenv ORAC_PERLBIN /star/Perl/bin/perl

alias oracdr_scuba source ${ORAC_DIR}/etc/oracdr_scuba.csh
```

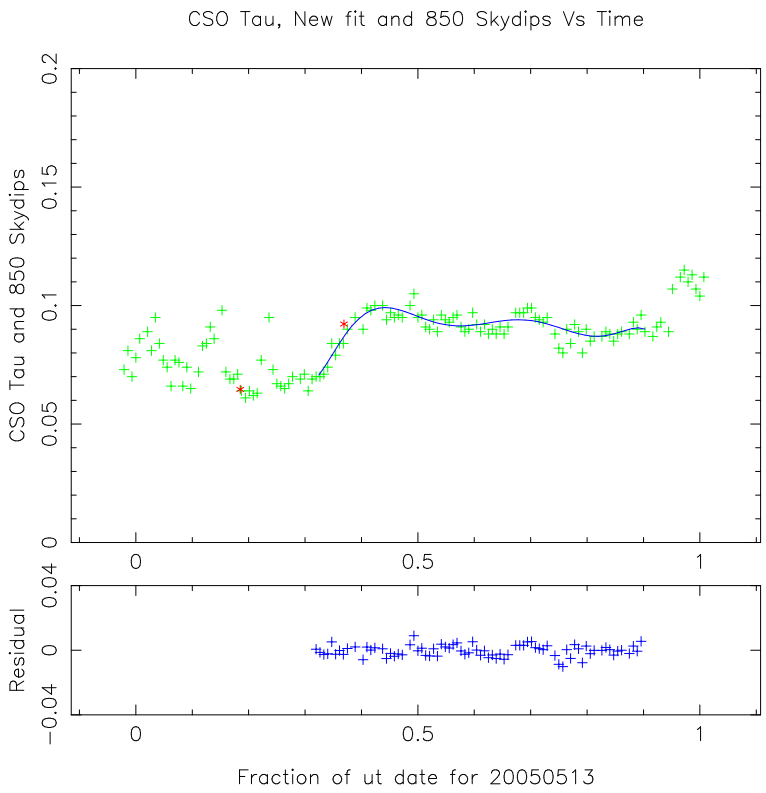

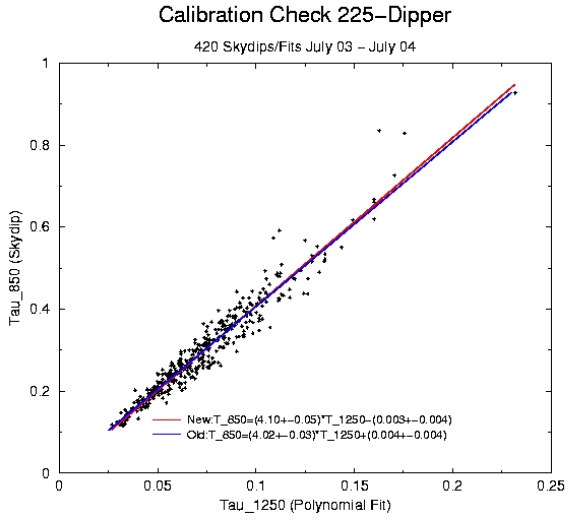

Figure 4.5: Top: the CSO sky opacity (green crosses) with the polynomial fit (blue line) and skydips (red asterisks); Middle: residuals of CSO fit; Bottom: a comparison of opacities derived from CSO and skydip data, which agree well (Archibald et al. 2002).

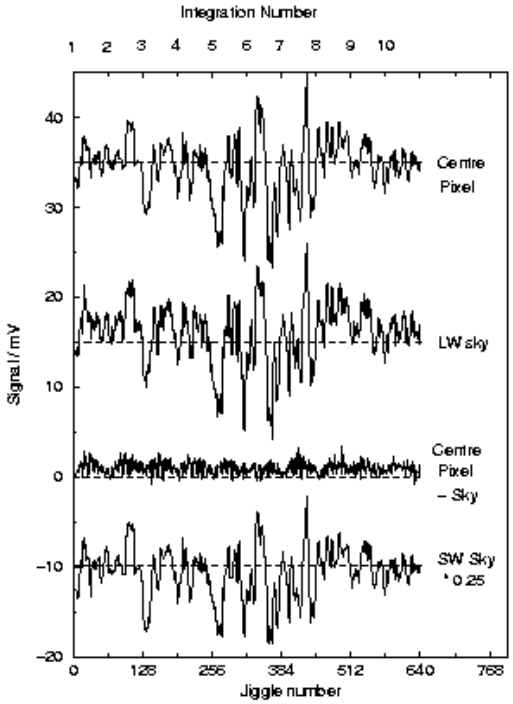

Figure 4.6: An effect of the sky noise removal: From the top: signal, sky, signal after sky removal, sky at 450 μm. The signal after subtraction is much more stable (Holland et al. 1999).

```
setenv CONVERT_DIR /d1/michal/oracdr/convert-1.5-5/

oracdr_scuba 20010912

setenv ORAC_DATA_IN /x/scr/michal/grb000210/20010912/raw
setenv ORAC_DATA_OUT /x/scr/michal/grb000210/20010912/reduced

oracdr -file list -cal tausys=csofit
```

They set a directory where `ORAC-DR` and `perl` environments were located, a UT date of observations and a directory of raw and reduced data. The last command executed the program reducing all observations with names specified in a file `list`, using CSO polynomial fits as an estimate of the atmospheric opacity. A more detailed description of each command can be found in the `ORAC-DR` User Manual[5].

[5] `http://docs.jach.hawaii.edu/star/sun231.htx/sun231.html`

As an output program returned the flux value (in mJy) averaged over all observations of a given source and the corresponding error. The results are summarized in Table 4.1. They all agree with those obtained by Tanvir et al. (2004) and Smith et al. (2005). The differences arise from possible slight changes in the reduction process and assumed conversion factors. Most sources were not detected in either 850 μm or 450 μm except of those marked as bold.

GRB host	850 μm [mJy] Literature	850 μm [mJy] My work	450 μm [mJy] My work
970228	0.20 ± 0.81	-1.13 ± 0.82	2.07 ± 7.93
970508	-1.57 ± 1.01	-1.53 ± 1.05	18 ± 30
970828	1.26 ± 2.36	0.86 ± 2.35	8 ± 17
971214	0.49 ± 1.11	-0.06 ± 1.24	-40 ± 23
980326	-0.27 ± 1.18	0.70 ± 1.28	-12.8 ± 13.5
980329	0.71 ± 0.69	0.60 ± 0.69	13 ± 10
980613	$\mathbf{1.75 \pm 0.92}$	$\mathbf{1.86 \pm 0.98}$	35 ± 27
980703	-1.53 ± 0.72	-1.59 ± 1.19	1.58 ± 9.52
981226	-2.79 ± 1.17	-1.58 ± 2.27	7 ± 10
990123	0.47 ± 0.60	-7.39 ± 4.37	20 ± 37
990308	0.02 ± 1.75	0.41 ± 1.48	-11.3 ± 6.1
990506	-0.25 ± 1.36	0.94 ± 1.55	-0.39 ± 24.56
991208	0.34 ± 0.83	0.42 ± 0.80	8.9 ± 8.0
991216	0.47 ± 0.94	0.79 ± 1.02	-3.3 ± 29.7
000210	$\mathbf{3.05 \pm 0.76}$	$\mathbf{2.81 \pm 1.03}$	-5.73 ± 30
000301C	-1.46 ± 0.90	-0.99 ± 0.89	-8.21 ± 4.65
000418	$\mathbf{3.15 \pm 0.90}$	$\mathbf{2.98 \pm 0.90}$	69 ± 166
000926	1.40 ± 1.23	1.14 ± 1.19	4.1 ± 7.9
001025A	-2.53 ± 3.04	0.60 ± 3.07	29 ± 21
010222	$\mathbf{3.74 \pm 0.53}$	$\mathbf{3.31 \pm 0.60}$	1.23 ± 28
010921	0.46 ± 1.14	-0.36 ± 1.11	-14 ± 9
011211	1.94 ± 0.89	2.07 ± 1.58	-16 ± 33
020813	-1.40 ± 3.50	-1.91 ± 2.07	-3.2 ± 13.8
021211	0.3 ± 1.9	-9.68 ± 8.34	8 ± 35
030115	0.2 ± 1.8	4.74 ± 4.85	-20 ± 42
030226	-0.1 ± 0.8	-0.81 ± 1.10	6 ± 9

Table 4.1: Results of the reduction of SCUBA photometry observations of GRB hosts: 850 μm flux found in the literature — mostly from Tanvir et al. (2004) and from Smith et al. (2005) for GRB 021211, GRB 030115 and GRB 030226 — and my own results. Bold — the only detections.

Chapter 5

Long-Wavelength Model

5.1 Description

In order to investigate the features of the Spectral Energy Distribution (SED) at longer wavelengths ($\lambda > 50\,\mu$m) covering far-infrared (FIR) to radio, I used the model developed by Yun & Carilli (2002). Their idea is to add contributions of different emission mechanisms, which are well understood and described quantitatively. They included thermal dust emission, thermal bremsstrahlung (free-free) emission and non-thermal synchrotron emission. In the following sections I will describe the emission mechanisms separately and then present the combined model.

5.1.1 Dust Emission

The flux density S_d emitted by a dust cloud with a temperature T_d can be represented by modified black body-curve

$$S_d(\nu) \propto Q(\nu)B(\nu, T_d) \tag{5.1}$$

where ν is the frequency, $B(\nu, T)$ is a black-body Planck curve

$$B(\nu, T) = \frac{2h}{c^2}\frac{\nu^3}{\exp(h\nu/kT) - 1} \tag{5.2}$$

h, c and k are the Planck constant, the speed of light and the Boltzmann constant, respectively. Q is an emissivity curve, which suppresses the black-body curve for $\nu < \nu_c$ (when cloud is optically thin) and is given by

$$Q(\nu) = 1 - \exp\left[-\left(\frac{\nu}{\nu_c}\right)^{\beta}\right] \tag{5.3}$$

where $\beta = 0 - 2$ is an emissivity index.

Dust emission is proportional to heating intensity of hot OB[1] newly born stars. The amount of dust is usually correlated with the SFR because new stars are born in dusty molecular clouds. Hence, Yun & Carilli (2002) found that the flux density observed at frequency ν_{obs} is proportional to the SFR and is given by

$$S_d(\nu_{\rm obs}) = 1.3 \cdot 10^{-6} \frac{{\rm SFR}(1+z)\nu_{\rm em}^3}{D_L^2(e^{0.048\nu_{\rm em}/T_d} - 1)}[1 - e^{-(\nu_{\rm em}/\nu_c)^\beta}] \quad [{\rm Jy}] \tag{5.4}$$

where $\nu_{\rm em} = (1+z)\nu_{\rm obs}$ is the galaxy rest frame frequency in GHz, SFR is the star formation rate for massive stars ($M > 5M_\odot$) in $M_\odot$/yr and D_L is a luminosity distance in Mpc. The flux is measured in units called janskys defined as 1 Jy $= 10^{26}$ watt per square meter per hertz.

5.1.2 Free-Free Emission

Free-free emission originates in an electron-photon scattering in ionized `HII` regions surrounding hot young stars. It depends on a thermal distribution of the electrons (with temperature T_e) and a free-free optical depth $\tau_{\rm ff}$ in the following way:

$$S_{\rm ff}(\nu) \propto B(\nu, T_e)(1 - e^{-\tau_{\rm ff}}) \tag{5.5}$$

A normalization factor can be derived from the SFR because it governs the production rate of the Lyman continuum photons and only hot stars can ionize the medium around them. The results can be written as

$$S_{\rm ff}(\nu_{\rm obs}) = 0.71\nu_{\rm em}^{-0.1} \frac{{\rm SFR}(1+z)}{D_L^2} \quad [{\rm Jy}] \tag{5.6}$$

5.1.3 Synchrotron Emission

Synchrotron emission comes from relativistic electrons emitted by supernova remnants and spiralating in their magnetic fields. A supernova rate (SNR) and in turn a supernova remnant rate are closely related to the SFR so the flux density of synchrotron emission is given by

$$S_{\rm nth}(\nu_{\rm obs}) = 25 f_{\rm nth}\nu_{\rm em}^{-\alpha} \frac{{\rm SFR}(1+z)}{D_L^2} \quad [{\rm Jy}] \tag{5.7}$$

$f_{\rm nth}$ is a factor of the order of unity and accounts for possible changes in proportionality between SNR and SFR. $\alpha = 0.7 - 0.8$ is a synchrotron spectral index.

[1] stars are divided into spectroscopical class denoted by letters OBAFGKM with temperature decreasing from O to M

5.1.4 Total Emission

Spectral Energy Distribution is constructed by combining all of these three contributions — adding equations (5.4), (5.6) and (5.7), which gives

$$S(\nu_{\rm obs}) = \left\{ 25 f_{\rm nth} \nu_{\rm em}^{-\alpha} + 0.71 \nu_{\rm em}^{-0.1} + 1.3 \cdot 10^{-6} \frac{\nu_{\rm em}^3 [1 - e^{-(\nu_{\rm em}/\nu_c)^\beta}]}{e^{0.048 \nu_{\rm em}/T_d} - 1} \right\} \times \times \frac{\mathrm{SFR}(1+z)}{D_L^2} \quad [\mathrm{Jy}] \tag{5.8}$$

Relative contributions vary with wavelength e.g. in the radio cm domain synchrotron radiation dominates whereas in FIR only the thermal emission of dust is non-negligible. It is illustrated on Figure 5.1 (Condon 1992).

Although all three discussed mechanisms are connected to the SFR, this statement should be assessed with some care. Since the lifetime of massive stars is $\sim 10^7$ years and the lifetime of synchrotron electrons is $\sim 10^8$ years, radio emission traces instantaneous SFR whereas submm emission traces the SFR integrated from the formation of the galaxy, because dust reprocess the starlight in much longer timescales (Condon 1992; Berger et al. 2001b; Berger 2003).

5.1.5 Mass of Dust

In the submm wavelengths the emission from dust is dominant (Figure 5.1), so the total dust mass, M_d, in a galaxy can be estimated using the submm flux. Taylor et al. (2005) found the following formula based on formalism developed by Hildebrand (1983):

$$M_d = \frac{S_\nu D_L^2}{(1+z)\kappa(\nu) B(\nu, T)} \tag{5.9}$$

where S_ν is the observed flux at the wavelength corresponding to a rest wavelength of $450\,\mu$m interpolated from the SED, ν is a rest frequency equal to 666.21 GHz ($450\,\mu$m), D_L is the luminosity distance in meters and κ is a mass absorption coefficient given by

$$\kappa(\nu) = 0.067 \left(\frac{\nu\,[\mathrm{GHz}]}{250} \right)^\beta \quad [\mathrm{m}^2/\mathrm{kg}] \tag{5.10}$$

and $B(\nu, T)$ is the Planck function.

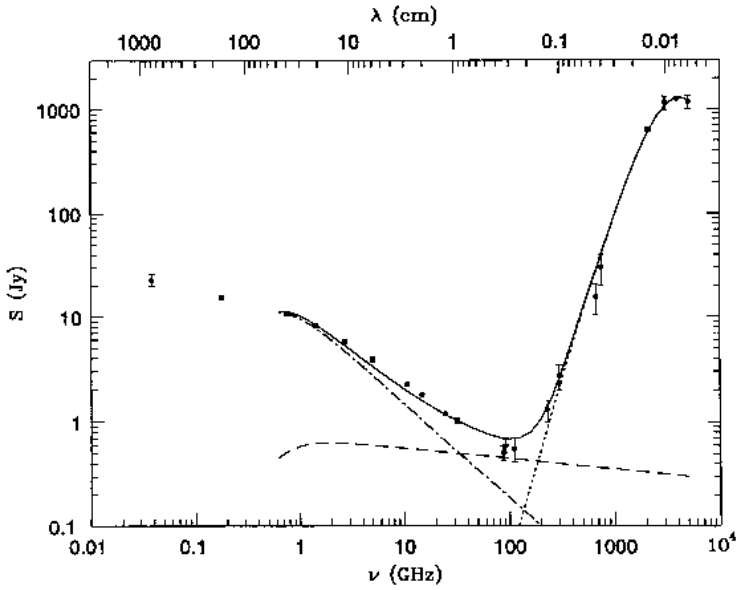

Figure 5.1: The SED of M82 (Condon 1992): data points and the models for different emission mechanisms: dust (dotted line), free-free (dashed line), synchrotron (dot-dashed line) and the sum (solid line). Different domains are dominated by different mechanisms

5.2 Data

I chose to analyse SEDs of GRB host galaxies for which at least 3 detections in the FIR to radio domain were available. Table 5.1 shows values of the flux density $S_\nu(\nu)$ collected from the literature and those resulting from my own reduction.

5.3 Method

For a given redshift and assumed cosmology ($\Omega_m = 0.3$, $\Omega_\Lambda = 0.7$, $H_0 = 72$ km/s/Mpc), equation (5.8) has 6 free parameters: $f_{\rm nth}$, α, ν_c, β, T_d and SFR, so fitting it to photometric data requires at least 7 datapoints in the FIR to radio domain (preferably more). Unfortunately such extended dataset does not exist for any of the GRB host galaxies. Hence, the only possible approach is to set several parameters to a constant value choosing those which are known not to vary a lot in larger galaxy samples. I assumed $f_{\rm nth} = 1$ for a Galactic normalization of the SNR vs. the SFR; $\alpha = 0.75$ because usually it has a value between 0.7 and 0.8; $\nu_c = 2 \cdot 10^{12}\,\mathrm{Hz}\,(150\,\mu\mathrm{m})$ for starburst

GRB host	z	450 μm [mJy]	Ref	850 μm [mJy]	Ref	8.46 GHz [μJy]	Ref	4.86 GHz [μJy]	Ref	1.43 GHz [μJy]	Ref
970508	0.84	18.0	1	−1.57	1,2	121.4	6	178.9	6	278.0	6
±		30.0		1.01		10.4		10.0		12.7	
980703	0.97	1.58	1	−1.53	1, 2	39.3	3	42.1	3	68.0	3
±		9.5		0.72		4.9		8.6		6.6	
000210	0.85	−5.73	1	3.05	1, 2	18.0	4			80.0[a]	4
±		30.0		0.76		9.0				52.0	
000418	1.12	69.0	1	3.15	1, 2	51.0	4	46.0	4	69.0	4
±		167.0		0.9		12.0		13.0		15.0	
010222	1.48	1.23	1	3.74	1, 2	17.0	4	19.0	4		
±		27.75		0.53		6.0		10.0			

GRB host	60 μm [mJy]	Ref	90 μm [mJy]	Ref	160 μm [mJy]	Ref	1350 μm [mJy]	Ref
970508	43.0	7	19.0	7	< 130.0	7	0.0	8
±	13.0		7.0				10.0	

GRB host	1.2 mm [mJy]	Ref	3.2 mm [mJy]	Ref	3.9 GHz [mJy]	Ref	0.61 GHz [mJy]	Ref
010222	1.05	5	−0.42	9	< 5.0	9	< 1.0	9
±	0.22		0.23					

Table 5.1: Long-wavelength photometric data for GRB host galaxies. References: 1: my own reduction, 2: Tanvir et al. (2004), 3: Berger et al. (2001b), 4: Berger et al. (2003), 5: Frail et al. (2002), 6: Frail et al. (2000), 7: Hanlon et al. (2000), 8: Smith et al. (1999), 9: Sagar et al. (2001).

[a] $\nu = 1.39$ GHz

galaxies (Scoville et al. 1991; Solomon et al. 1997). The rest of the parameters (β, T_d and SFR) were changed to obtain the best fit.

The SFR given by equation (5.8) refers to the formation rate of massive stars with masses $M > 5M_\odot$ because only those stars heat up the dust significantly (dust emission), emit Lyα photons, and ionize the medium (free-free emission), and end their lives as supernovae (synchrotron emission). In order to transform it to the total SFR (the formation rate of all stars) some initial mass function (IMF) must be assumed. I considered a Salpeter IMF (Salpeter 1955). It gives total mass of stars dN (number of stars times their mass) in a given mass bin from M to $(M + dM)$:

$$dN = AM^{-\alpha}dM \tag{5.11}$$

where A is a constant and the exponent is assumed to be $\alpha = 1.35$. Because an integral over all masses is

$$\int_{M_{\rm min}}^{M_{\rm max}} dN = \frac{A}{1-\alpha} M^{1-\alpha}\Big|_{M_{\rm min}}^{M_{\rm max}} \tag{5.12}$$

then the conversion factor between the SFR of massive stars and the total SFR is

$$\frac{\int_{M_{\rm min}}^{M_{\rm max}} dN}{\int_{5M_\odot}^{M_{\rm max}} dN} = \frac{M_{\rm max}^{1-\alpha} - M_{\rm min}^{1-\alpha}}{M_{\rm max}^{1-\alpha} - 5^{1-\alpha}} = 5.51433 \tag{5.13}$$

where a numerical value was obtained by choosing $M_{\rm min} = 0.1M_\odot$ and $M_{\rm max} = 100M_\odot$ (Berger et al. 2001b).

I performed the χ^2 minimization fit of the function given in equation (5.8) to data from Table 5.1 using the `CURVEFIT` `IDL`[2] routine.

5.4 Results and Discussion

5.4.1 The Fit

As expected from Figure 5.1 and equation (5.8), the SFR (the scaling factor of this equation) was mostly constrained by radio (synchrotron) detections, regardless of dust properties. Then T_d and β could be found by fitting submm and FIR parts of the spectrum. SEDs of GRB hosts were not well-sampled so I needed to do further simplifications depending on number of available

[2]Interactive Data Language

datapoints. For GRB 980703 only radio detections existed, so I fixed $T_d = 58$ K and $\beta = 1.35$ (Yun & Carilli 2002). For GRB 970508, GRB 000210 and GRB 000418 there was only one FIR or submm detection which did not give a possibility to fit both T_d and β simultaneously without ambiguity. Hence, I chose $\beta = 1.35$, except of the case of GRB 970508 for which $\beta = 2.0$ had to be chosen in order for a submm upper limit to be consistent with the fit. Only for GRB 010222 both submm and mm data were available, so I could fit all three parameters simultaneously.

Figure 5.2 and Table 5.2 show the best fits and fitting parameters. An inspection by eye of the plots confirms the fact that the SEDs of GRB hosts are well represented by equation (5.8). A high value of χ^2 for GRB 970508, GRB 980703 and GRB 000418 can be explained by choosing too high synchrotron spectral slope α. However, changing this parameter did not influence the other parameters, most importantly the SFR. Fits of GRB 000210 and GRB 010222 gave fairly small $\chi^2 < 1$, which could indicate that the error bars of the datapoints were too large (or that the datapoints are not gaussianic distributed around the analytical value). Indeed, the radio detections for these GRB hosts were very weak ($2 - 3\sigma$).

All submm upper limits were consistent with the fit. It was not surprising because 850 μm detections were very weak, so 3σ upper limits for 450 μm were above the curve, given that the 450 μm SCUBA array is less sensitive than the 850 μm one. For GRB 000210 and GRB 010222 the 450 μm upper limits were not far above the model which gives the chance to detect these galaxies with increased integration time and/or telescope class. The only inconsistent upper limit was at 90 μm for GRB 970508. Its flux was smaller than neighboring 60 μm point. In this range the spectrum decreases with frequency so it was impossible to get consistency with this limit, unless a very high temperature ($\sim$ 300 K) was chosen, which would shift the dust emission peak to a wavelength shorter than 90 μm. However, in such a case it was impossible to fit both radio and IR parts reasonably.

I checked if submm observations of GRB hosts did not suffer from so-called confusion. It may arise from a coarse resolution of the submm receiver — other sources can fall into the SCUBA main beam. Confusion limits are equal to 2 mJy for 850 μm and 14 mJy for 450 μm (Blain et al. 1998). Hence, the confusion limits were not reached because they were located below the model curve (Figure 6.3).

A plateau at high frequencies for GRB 970508 and GRB 980703 (Figure 5.2) were only numerical artifacts. Dust thermal emission at these frequencies was so small that the program could not handle it and set the value to $\sim 10^{-6}$ Jy.

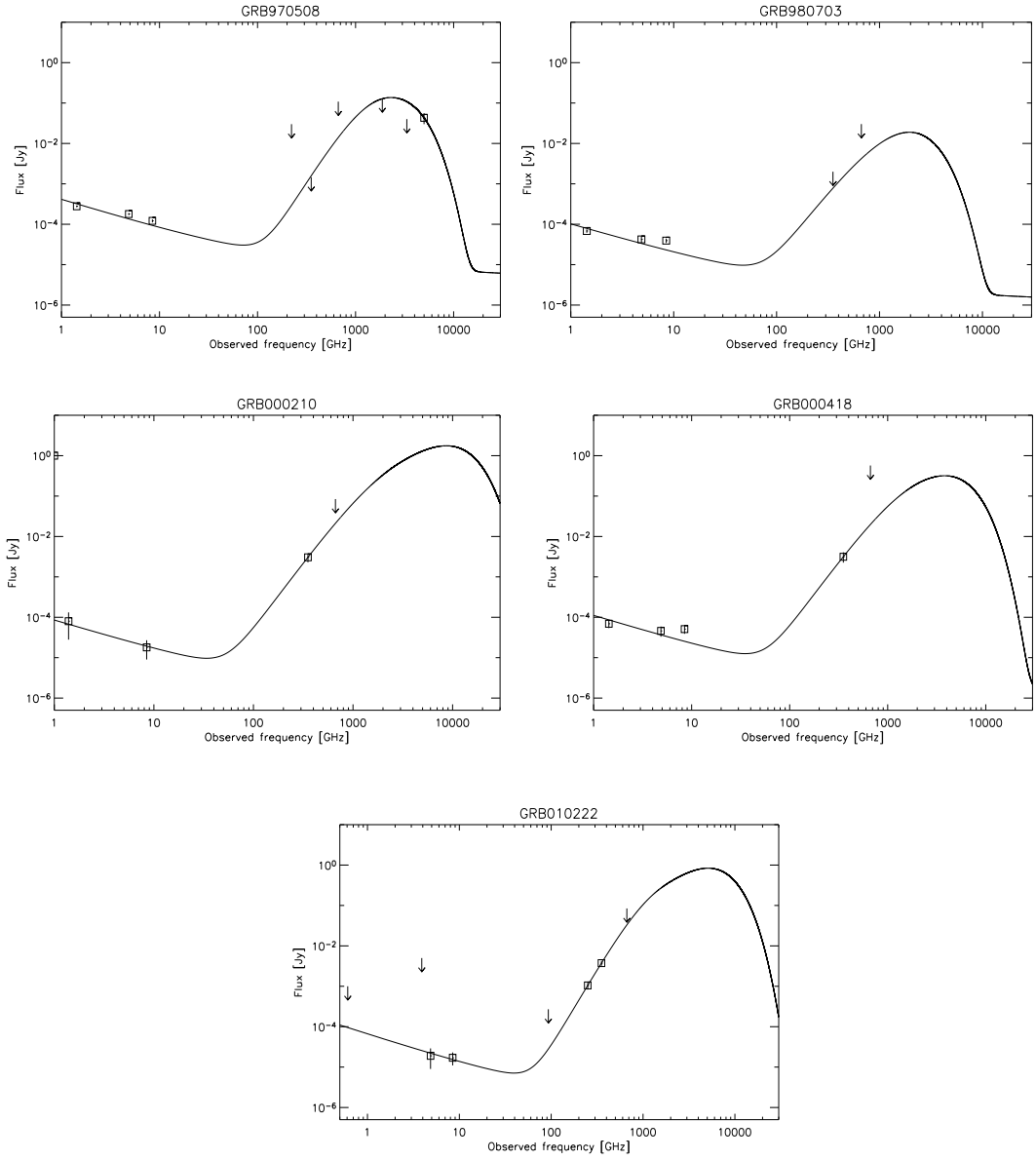

Figure 5.2: Fits of the function defined by Yun & Carilli (2002) to the SEDs of GRB hosts. Squares are detections and arrows are 3σ upper limits.

GRB host	$SFR_{FIR-radio}$ $[M_\odot/yr]$	T_d [K]	β	χ^2/dof	SFR_{UV} $[M_\odot/yr]$	Ref	M_d $[10^7 M_\odot]$
970508	2077 ± 69	69 ± 3	2.00 (fixed)	9.13	0.25	1	3.5
980703	695 ± 52	58 (fixed)	1.35 (fixed)	2.42	$8 - 13$	2	4.3
000210	428 ± 171	272 ± 121	1.35 (fixed)	0.04	2.1 ± 0.2	3	2.6
000418	1062 ± 158	137 ± 39	1.35 (fixed)	1.59	6.2 ± 0.2	4	6.6
010222	1211 ± 358	215 ± 125	1.92 ± 0.65	0.17	1.5	5	2.4

Table 5.2: Fitting parameters (SFR, T_d and β) of the function of Yun & Carilli (2002) and χ^2 per degree of freedom. SFRs derived from UV continuum (no extinction correction) are given for comparison along with references: 1: Bloom et al. (1998), 2: Holland et al. (2001), 3: Gorosabel et al. (2003a), 4: Gorosabel et al. (2003b), 5: Berger et al. (2003). Finally, the derived mass of dust (equation (6.1)) is presented.

5.4.2 SFR

Derived SFRs of the order of several hundreds $M_\odot$/yr indicate that GRB hosts are highly star-forming galaxies. A usual value found at similar redshift is not more than $100 M_\odot$/yr for a mid-IR *Spitzer* selected sample of 747 galaxies (Caputi et al. 2006, Figure 9 therein). However, for galaxies found in submm searches SFRs are similar to those derived here (Scott et al. 2002, Tables 9 and 10 therein). Both authors estimated SFR in the same way from infrared luminosities (equation (6.2)). Scott et al. (2002) based their estimates only on submm data and extrapolated it using a gray-body spectrum (equation (5.4)). Radio selected galaxies have also high values of SFR $\sim 1000 M_\odot$/yr as reported by Haarsma et al. (2000). Hence, GRB hosts presented here seem to resemble the properties of a submm/radio rather than an IR selected sample. However, this is not true for a GRB host sample as a whole, which are rather blue, subluminous galaxies without pronounced submm emission (Le Floc'h et al. 2003; Tanvir et al. 2004). It is then probable that GRB hosts presented here represent either the bright-end or the most dusty (unlikely, because hosts are blue) or the youngest (see Chapter 7) part of the whole sample.

As the SFR for GRB 970508 was extremely high I suspected that there was a significant contamination from the afterglow in the data. I re-investigated radio observations from Frail et al. (2000). Previously I averaged the detections later than 200 days after the burst and assumed that this value represented the host emission. In order to check this assumption I fitted a power-law (equation (2.1)) to all of the afterglow datapoints which showed a

decline and determined the flux of the galaxy $f_{\rm gal}$. An example is presented in the upper panel of Figure 5.3. As it is shown on the lower panel of the same figure, the fit was rather consistent with an unphysical negative value of the galaxy flux (the smallest χ^2) so the conclusion is, that in these observations the host was not detected, and the result for GRB 970508 in Table 5.2 are not reliable because the data contained mainly the afterglow signal.

In Table 5.2 the SFRs derived from the UV continuum are shown (method described by Kennicutt 1998). They are $2-3$ orders of magnitude less than what I derived based on FIR to radio observations. It suggests that the majority of UV light is obscured by dust present in the host (Berger et al. 2003) what is not surprising because they are highly star-forming galaxies. However, even after applying extinction correction, the UV-based SFRs were still much lower than the FIR to radio based SFRs, e.g. values of UV-based SFRs were $65-100 M_{\odot}$/yr for GRB 980703 with somewhat high extinction $A_V = 2.2$ (Holland et al. 2001) and $70.1 \pm 33.7 M_{\odot}$/yr for GRB 000418 with $A_V = 1.47$ (Gorosabel et al. 2003b). The results based on other optical indicators such as strength of line [O II] (described in Kennicutt 1998; Piro et al. 2002) were similarly small comparing to long-wavelength data. To explain this discrepancy Gorosabel et al. (2003a) proposed that, at least in the case of GRB 000210, the host was very clumpy and contained two separate populations of massive stars: one traced by the UV / optical observations with no sign of extinction and the other completely obscured by dust which re-emitted in longer wavelength. A similar hypothesis in general was discussed by Bressan et al. (2002). They claimed that the UV light of young galaxies was dominated by old stars because the young stars were embedded in dense molecular clouds which absorbed optical light. Then of course UV is not a good tracer of star-formation and UV indicators gives a smaller value of the SFRs which can be interpreted as lower limits.

5.4.3 Dust Properties

The dust temperatures derived from the fit were much higher than those found in submm searches at a variety of redshift. For example Blain et al. (2004) obtained a range $T_d = 10-60$ K for dust-enshrouded galaxies up to redshift $z \sim 1.3$, and Blain et al. (1999b) noticed that SEDs of SCUBA galaxies were consistent with $T_d \sim 40$ K. Moreover, Taylor et al. (2005) reported average dust temperatures equal to 40 K and 24 K for starburst- and quiescent galaxies, respectively. The limited sample and the limited wavelength coverage for each host galaxy discussed here did not allow me to draw any statistically confident conclusion from high dust temperatures of GRB hosts. However, if such a result was common for other hosts and for

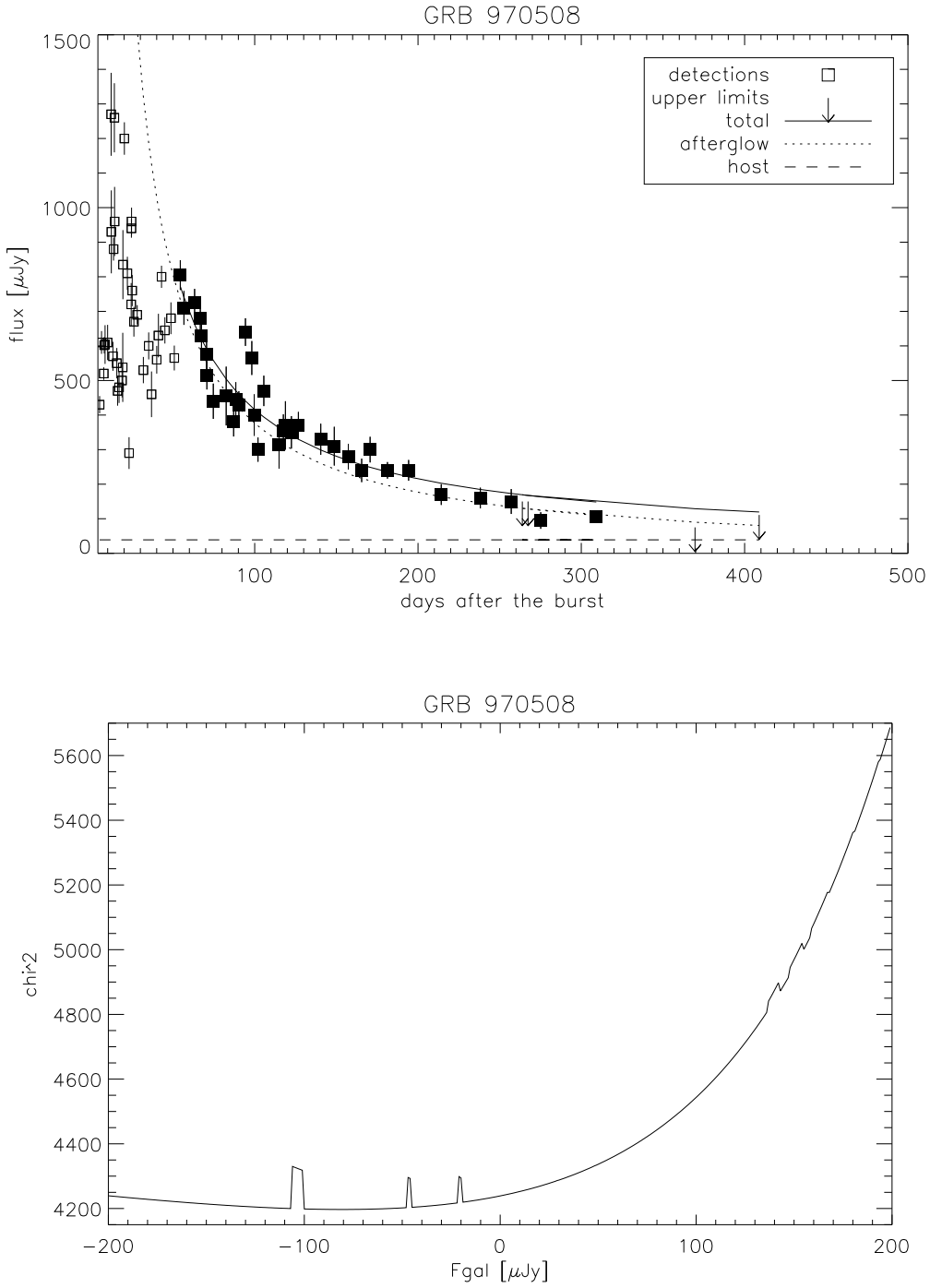

Figure 5.3: Top: the fit of the power-law to the radio afterglow of GRB 970508 (data from Frail et al. (2000)). Only filled squares were used in the fit. See inset for description of the symbols. Bottom: χ^2 as a function of the flux of the galaxy in the power-law fit to the afterglow. Since the best fit is represented by unphysical negative galaxy flux, the host was not detected.

better sampled SEDs it would imply very hot dust environments which can be interpreted as a high number of hot OB stars enshrouded by this dust, and hence young stellar populations with a significant amount of dust. High dust temperatures of GRB hosts could also explain their low detectability in submm, as in this case a dust peak is shifted towards shorter wavelengths (as also claimed by Priddey et al. 2006).

It was proposed in a numerical approach to the galaxy evolution performed by Totani & Takeuchi (2002, Figure 7 therein), that dust temperatures might be as high as 80 K in very young galaxies — up to several hundreds Myrs after formation. Even higher temperatures ($\sim$ 100 K) was obtained by the modeling of the dust evolution by Hirashita et al. (2002, Figure 3 therein). Finally, observational evidences of hot dust (80 K and 210 K components) in a young galaxy was found by Dale et al. (2001b). The low host ages is also proposed in Chapter 7.

Another explanation of high dust temperatures could be, that GRB hosts contain Active Galactic Nuclei (AGNs). Gillmon et al. (2006) reported $T \sim$ 100 K for AGNs observed in FIR, whereas several galaxies classified as AGNs detected in wavelengths from optical to millimeter by Klaas et al. (2001) had temperatures $\sim$ 70 K. However, AGN as a power source of GRB host emission is rather disfovoured by observational evidences (see Section 3.2).

As mentioned before, my estimation of dust temperatures is uncertain because there is a significant degeneracy between T_d and β (Dunne & Eales 2001) and their decoupling is difficult even for well-sampled spectra (Yun & Carilli 2002). It is because a shallower slope can mimic the effect of colder dust with a steeper slope (Bressan et al. 2002). However, even if the lowest possible $\beta = 0$ is assumed (optically-thick dust, black-body spectrum) derived temperatures were still high: 102 ± 44 K for GRB 000210 and 62 ± 14 K for GRB 000418. For GRB 010222 the dust temperature had to stay high because otherwise SED was not consistent with the submm to mm spectral slope.

In order to investigate how robust my results of high temperatures were, I investigated the χ^2 of the fit in a full $T - \beta$ parameter space. The results of the calculations are shown on Figure 5.4, namely a 3D plot of χ^2 as a function of the values of T and β used in the fit. A solid thick line follows the best value of β for each T. For all three host galaxies (GRB 000210, 00418 and 010222) low temperatures are ruled out by the data (see projections of thick curves on $\chi^2 - T$ planes). More precisely $T \gtrsim 80$ K for GRB 000210, $T \gtrsim 50$ K for GRB 000418 and $T \gtrsim 100$ K for GRB 010222.

The value of β was unconstrained except for GRB 010222 for which two data points were available in the submm to mm part of the spectrum. In this case χ^2 was minimal for $T = 215$ K and $\beta = 1.92$ as can be seen clearly

on the logarithmic version of Figure 5.4, on projections onto the $\chi^2 - T$ and $\chi^2 - \beta$ planes. On this figure thick lines on this figure tracing the best fits goes diagonally through the $T - \beta$ plane, so two possible extreme cases were possible: these GRB hosts were either optically thick ($\beta \sim 0$) with "lower" temperatures ($T \sim 100$ K) or they had a large spectral index ($\beta \sim 2$) and were significantly hot ($T \sim$ several $\times$ 100 K). The lower value of β accompanied by the high temperature or vice versa were ruled out.

Figure 5.5 shows the expected 850 μm fluxes assuming a wide range of temperatures. Observed fluxes with 1σ errors are plotted for comparison. I used $\beta = 0$ which gave the lowest and therefore the most robust lower limit to the temperature. The conclusion was similar to the one obtained from the analysis of χ^2: GRB host galaxies seems to have very high dust temperatures.

It must be pointed out that the lower limits on the temperatures was derived based only on one datapoint in a dust emission regime, what normally is not enough. I could do it because the function of Yun & Carilli (2002) assumed the radio-submm correlation (a proportionality of both fluxes to the SFR). This correlation is firmly established (van der Kruit 1973; Condon 1992; Helou & Bicay 1993; Yun et al. 2001; Garrett 2002) and it has already been used to derive dust temperatures based only on one submm and one radio detection by Chapman et al. (2003, 2005). The scatter of the relation is not very big — it varies not more than by a factor of 2 (Appleton et al. 2004). I have checked how big an error it introduce to the temperature estimation. I assumed the radio flux-SFR normalization to be twice smaller ($f_{\rm nth} = 0.5$ in equation (5.7)) and found out that this caused a decrease of the temperature by a factor of 1.7 and the increase of the SFR by a factor of 2. Hence, taking into account this uncertainty, the above lower limits transformed into $T \gtrsim 47$ K for GRB 000210, $T \gtrsim 29$ K for GRB 000418 and $T \gtrsim 59$ K for GRB 010222.

Results of the dust mass estimation using equation (5.9) are shown in the last column of Table 5.2. The dust masses were of the order of $10^7 M_\odot$ and agreed well with the average value of $5.5 \times 10^7 M_\odot$ for starburst galaxies found by Taylor et al. (2005).

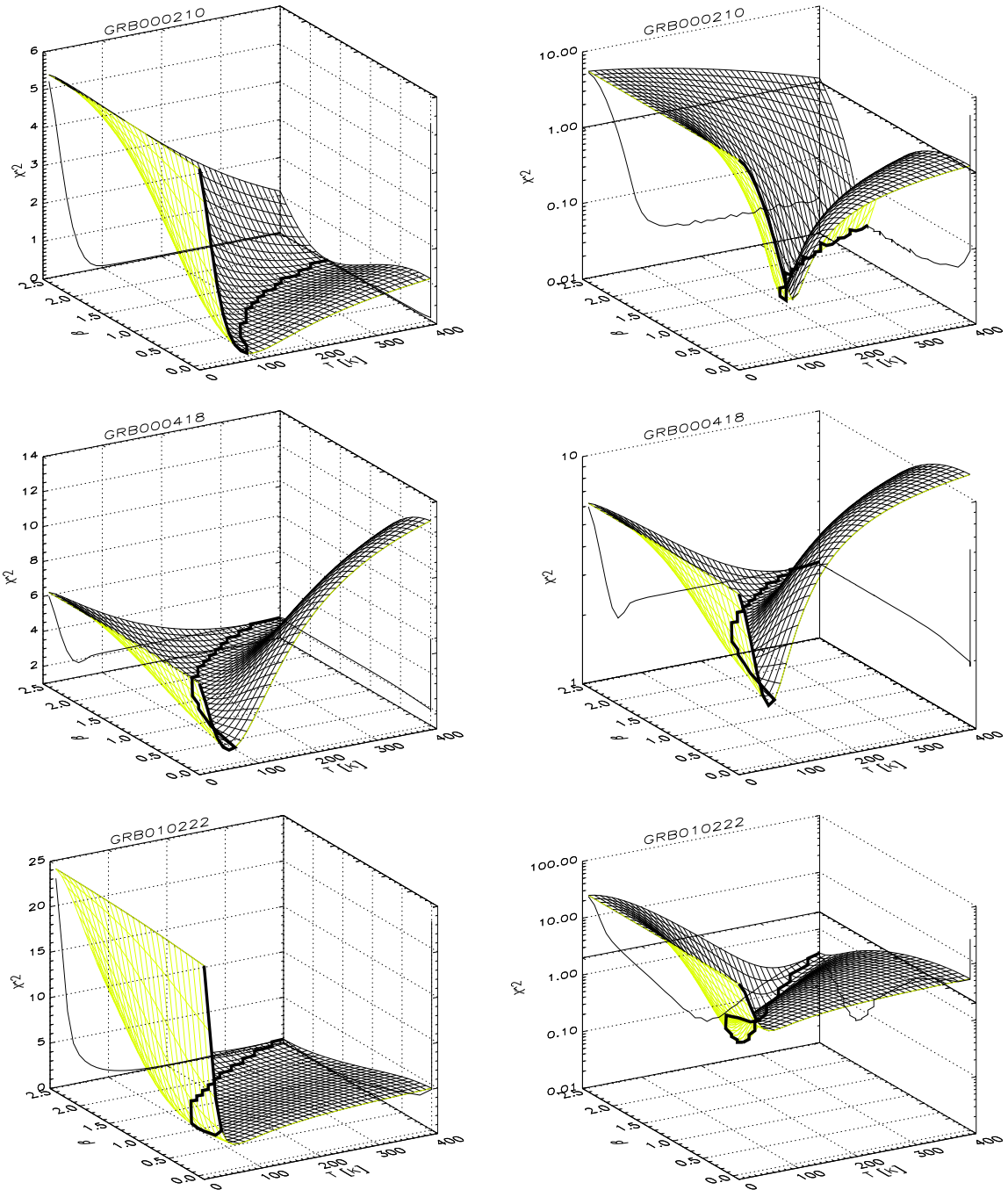

Figure 5.4: Surfaces: χ^2 for the whole $T - \beta$ parameter space in the Yun & Carilli (2002) function fitting. Thick lines: best fits for each temperature. Thin lines: projections of thick lines onto sidewalls. Left: linear χ^2 scale. Right: logarithmic χ^2 scale shown in order to display more clearly the "valleys" of the best fits.

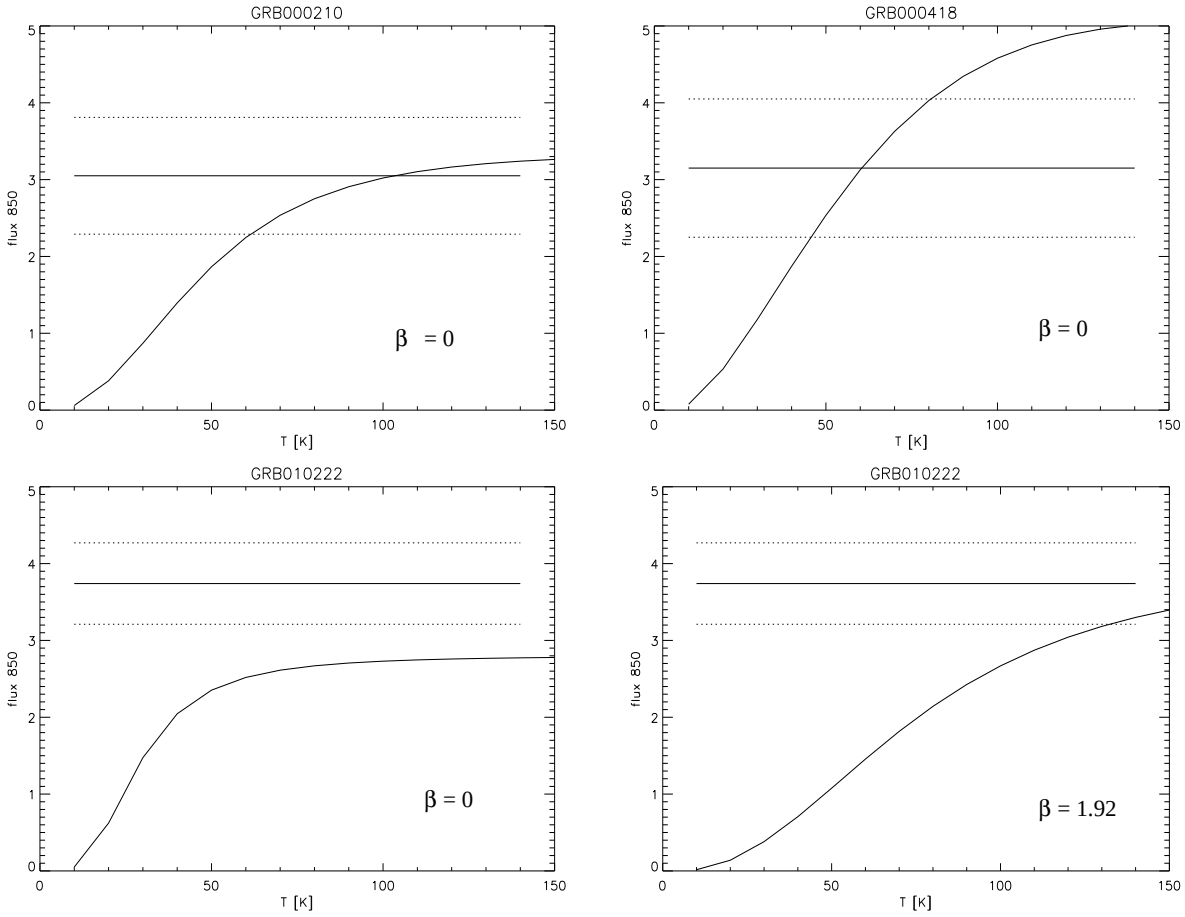

Figure 5.5: The expected fluxes at observed wavelength of 850 μm (solid curves) for different GRB hosts with different values of the spectral index β along with the observed fluxes (solid lines) and its 1σ errors (dotted lines).

Chapter 6

Entire Spectrum Model

6.1 Description

6.1.1 Spectral Energy Distribution

In order to consider data at shorter wavelengths (UV/optical/near-infrared) new sources of emission must be included, namely emission from hot stars themselves (not reprocessed by dust), higher temperature dust components, smaller grains, Polycyclic Aromatic Hydrocarbons (PAHs), etc. Unfortunately there is no simple solution to this issue so numerical calculations should be used.

One such approach was taken by Dale et al. (2001a) and Dale & Helou (2002). For a broad range of heating intensities ($U = 0.3 - 10^5$ in units of local interstellar radiation field) they combined the emission curves of three dust components: large grains (dust as in Chapter 5), very small grains and PAHs. They assumed a power-law distribution of dust mass over a range of heating intensities:

$$dM_d(U) \propto U^{-\alpha} dU, \tag{6.1}$$

and added contributions from different heating intensities. For a high value of α a distribution $M_d(U)$ is narrow, mostly concentrated at low heating intensities, what can be interpreted as low SFR because the number of hot, young stars is low. On the other hand, a small value of α means that a significant fraction of dust is bathed in intense radiation field, that is in an environment of hot, newly born stars, what implies a high SFR.

The resulting SED has a range $\lambda = 3 - 1100\,\mu$m. The optical starlight down to $0.36\,\mu$m as well as the radio synchrotron part up to 22.5 cm (equation (5.7)), are added.

6.1.2 Star Formation Rate

Having an SED of this range it is possible to calculate the SFR by equation (Kennicutt 1998):

$$\mathrm{SFR}\,[M_\odot/\mathrm{yr}] = A \cdot 10^{-44} L_{IR}\,[\mathrm{erg/s}], \tag{6.2}$$

where L_{IR} is the infrared luminosity integrated over the wavelength range $8-1000\,\mu$m (rest frame) and A is a numerical constant of order unity. Kennicutt (1998) found $A = 4.5$; this is towards the lower limit of an empirical value derived by Buat & Xu (1996), $A = 8^{+8}_{-3}$, based on studies of 152 disk galaxies of type Sb or later. I used the former estimation because it is standard and widely applied. Ranges given by Buat & Xu (1996) indicate that SFR estimation is uncertain by a factor of a few.

6.2 Data

I supplemented the photometric data of GRB hosts from my sample (Table 5.1) with the optical/near- and mid- infrared observations summarised in Table 6.1. The first part of the table gives apparent Vega magnitudes, or fluxes, in different filters with references. For GRB 970508, GRB 000210 and GRB 000418 there are real host detections achieved by observations of the galaxies long after the GRB events, and for GRB 980703 and GRB 010222 the data resulted from the fitting of the GRB afterglow lightcurves and the determination of underlying galaxy components (equation 2.1).

Magnitudes needed to be transformed into fluxes except for GRB 970508 and GRB 010222 for which quoted values were already in μJy. For GRB 980703 I applied the photometric calibration described by Bessell (1979) for V, R and I filters and by Bessell & Brett (1988) for J, H and K. Namely, for each filter I retrieved the values of the flux f_0 in janskys for a fiducial star of magnitude mag_0 (Table 6.2) and calculated the flux of the galaxy f with magnitude mag using

$$f = f_0 \cdot 10^{0.4(\mathrm{mag}_0 - \mathrm{mag})}. \tag{6.3}$$

For GRB 000210 and GRB 000418 the authors published offsets to AB magnitudes, what enabled me to calculate the flux using the following formula[1]:

$$f = 10^{0.4(8.9 - \mathrm{mag}_{AB})} \quad [\mathrm{Jy}]. \tag{6.4}$$

The second part of Table 6.1 contains *Spitzer* mid-infrared data (Castro Cerón et al. 2006; Le Floc'h et al. 2006). Upper limits are 3σ.

[1] www.astro.livjm.ac.uk/~ikb/convert-units/node1.html

GRB host	U [mag]	B [mag/ μJy]	V [mag/ μJy]	R [mag/ μJy]	I [mag/ μJy]	Z [mag]	J [mag]	H [mag]	K [mag]	Ref	$4.5\mu m$ [μJy]	$8\mu m$ [μJy]	$24\mu m$ [μJy]	Ref
970508[a]		0.20	0.28	0.30	0.56					1	< 3.1	< 17.2	< 82	6
$\pm$		0.04	0.07	0.05	0.15									
980703			23.04	22.58	21.95		20.87	20.27	19.62	2	11.1	< 23.5	< 83	6
$\pm$			0.08	0.06	0.25		0.07	0.19	0.12		2.1			
000210	23.54	24.40	24.22	23.46	22.49	22.83	21.98	21.51	20.94	3				
$\pm$	0.13	0.13	0.08	0.1	0.12	0.28	0.1	0.23	0.14					
000418	23.54	24.07	23.8	23.76	23.39	22.79	22.46	22.27	21.19	4				
$\pm$	0.3	0.05	0.06	0.1	0.05	0.05	0.1	0.1	0.3					
010222[a]		0.109	0.103	0.063	0.119					5	< 3.0	< 21.1	< 81	7
$\pm$		0.014	0.011	0.008	0.027									

Table 6.1: Optical / infrared photometric data for GRB host galaxies in Vega magnitudes or μJy. References: 1: Sokolov et al. (2001), 2: Vreeswijk et al. (1999), 3: Gorosabel et al. (2003a), 4: Gorosabel et al. (2003b), 5: Galama et al. (2003), 6: Castro Cerón et al. (2006), 7: Le Floc'h et al. (2006). (The definitions of filters and their wavelengths differ for different authors).

[a]Flux is given in μJy for this GRB host

Filter	V	R	I	J	H	K
mag_0	0.0	0.0	0.0	0.03	0.03	0.03
f_0 [Jy]	3640	3080	2550	1570	1020	636

Table 6.2: Fluxes f_0 of fiducial star with magnitude mag_0 for each filter (Bessell 1979; Bessell & Brett 1988).

6.3 Method

Varying of the model parameters requires numerical computations and access to the model code. So I only examined those SEDs provided by Dale[2]. 64 SEDs were available, each characterised by the parameter α (equation (6.1)) with a range: $0.0625 - 4.0$.

I blueshifted the observational data into the galaxy rest frame by:

$$\nu_{\mathrm{em}} = (1+z)\nu_{\mathrm{obs}} \qquad \text{or} \qquad \lambda_{\mathrm{em}} = \frac{\lambda_{\mathrm{obs}}}{1+z}, \tag{6.5}$$

where the "em" subscript denotes emitted (galaxy rest frame) values and the "obs" one observed values.

Then I fitted the model of Dale et al. (2001a) to the data using the following procedure: for each wavelength corresponding to a datapoint (in the galaxy rest frame) I calculated the flux value in the model by integrating over the width of the filter. Then the model was scaled in order to match the data. These steps were repeated for each of the 64 models and the best fitting model was chosen.

The flux density f_ν was transformed to the luminosity density using equation (Hogg et al. 2002)[3]:

$$L_\nu(\nu_{\mathrm{em}}) = \frac{4\pi D_L^2}{1+z} f_\nu(\nu_{\mathrm{obs}}), \tag{6.6}$$

where D_L is the luminosity distance and the $1+z$ factor accounts for the fact that the flux and the luminosity are not bolometric but densities per unit frequency and the bandwidth $d\nu$ is reduced.

[2] `http://faraday.uwyo.edu/~ddale/research/seds/seds.html`

[3] See also a nice explanation in Section 8.2 on page 22 of
`http://www.roe.ac.uk/~ant/Teaching/Astro%20Cosmo/Cos4_0105.pdf`

GRB host	SFR_{IR} $[M_\odot/yr]$		χ^2/dof	
	$\alpha = 0.0625$	$\alpha = 4.0$	$\alpha = 0.0625$	$\alpha = 4.0$
970508	6.90	0.48	1.31	1.31
980703	126.23		10.65	
000210	22.48	1.57	8.49	8.48
000418	53.27	3.72	15.36	15.39
010222	6.77	0.47	4.88	4.88

Table 6.3: Results of the fitting of the model of Dale et al. (2001a) for two extreme values of α. For all but GRB 980703 the fitting to the optical/infrared data only are considered.

6.4 Results and Discussion

6.4.1 GRB 980703

The only case for which the model of Dale et al. (2001a) fitted both radio and optical data was GRB 980703, so it is discussed separately. The best fit is shown in Figure 6.1 along with the model of Yun & Carilli (2002) from Chapter 5 and the sensitivities of several telescopes in the FIR–radio range. The results for all hosts are summarised in Table 6.3.

The fit for GRB 980703 was good in terms of reproducing the SED trends though, statistically, χ^2 was high. A better match can probably be achieved by adding the dust extinction of the optical light. This would bring the optical part of the SED down. A problematic inconsistency with the data was the fact that one of the mid-IR upper limits was below the model. The model should be lowered by a factor of 6 to be consistent. This lowering indicates that, for this case, either a model with a steeper optical–FIR slope is needed, the dumping of PAHs (Dale et al. 2001a) should be stronger (PAH emission dominates in the mid-IR region), or the silicate absorption should be enhanced.

Since the model fitted well the radio part, the inferred SFR differed from the value obtained in Chapter 5 only by a factor of 5 (compare Tables 5.2 and 6.3). It is usual to observe scatter in the luminosity-SFR relation (Buat & Xu 1996), so it can be concluded that the normalisation of equations (5.8) is (6.2) are consistent and correct.

For the galaxy rest wavelength $\lambda > 100\,\mu$m both models of Yun & Carilli (2002) and Dale et al. (2001a) agreed well (Figure 6.1). There were however minor differences: the model of Dale et al. (2001a) had slightly larger spectral

index α (steeper radio spectrum) and higher temperature (the dust peak at shorter wavelength). The emissivity index β was the same because the models were parallel in the submm region.

6.4.2 Other GRB Hosts

As mentioned above, the model of Dale et al. (2001a) did not fit both the radio and optical observations of GRB 970508, GRB 000210, GRB 000418 and GRB 010222. Hence I fitted it only to optical/infrared data and calculated the SFRs from the infrared emission using equation (6.2). Since the index α parameter (equation (6.1)) influences only the mid-infrared to radio part of SED I could not distinguish between different models of Dale et al. (2001a), so I investigated both extreme cases: $\alpha = 0.0625$ and $\alpha = 4.0$. The fits and the results are presented in Figure 6.3 and Table 6.3.

For all but GRB 970508 fits were statistically poor (high χ^2) and only reproduced the trends in the optical SEDs, without matching the detailed behaviours. This was addressed in Chapter 7.

As seen in Figure 6.3, models with $\alpha = 0.0625$ (starburst) fitted better than models with $\alpha = 4.0$ (quiescent). This is because the discrepancy between optical and radio detections was larger in the latter case. However, in order to achieve full consistency, another physical mechanism must be included to bring down the optical emission in the model (e.g. gray extinction as claimed by Savaglio et al. 2003; Chen et al. 2006b) or to boost the radio emission (e.g. by adding an AGN component).

The SFRs derived fitting the model of Dale et al. (2001a) only to the optical/infrared data agreed well with those values based on the UV continuum (Tables 5.2 and 6.3). This is because both estimations were based on the same data. Moreover it confirmed the fact that the infrared part of the spectrum can be used (via equation (6.2)) even if only optical data are present. Of course the uncertainty is then bigger.

The case of GRB 970508 yielded meaningful values, unlike those in Table 5.2, because here it was based on optical observations of the host without afterglow contamination.

Figures 6.1 and 6.3 show the sensitivities of *Spitzer*, SCUBA and the Plateu de Bure Interferometer (PdBI). Assuming that the model of Yun & Carilli (2002) is correct then all described GRB hosts are bright enough to be detected by *Spitzer* and, at the shortest wavelength (1.2 mm), by the PdBI.

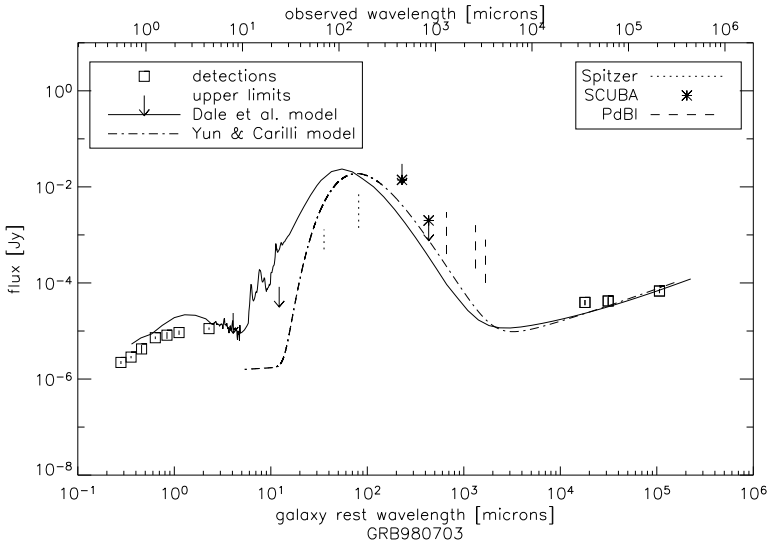

Figure 6.1: The model of Dale et al. (2001a) fitted to the observations of GRB 980703 host together with upper limits, the model of Yun & Carilli (2002, see Chapter 5) and sensitivities of several telescopes. (See insets for a description of the symbols.)

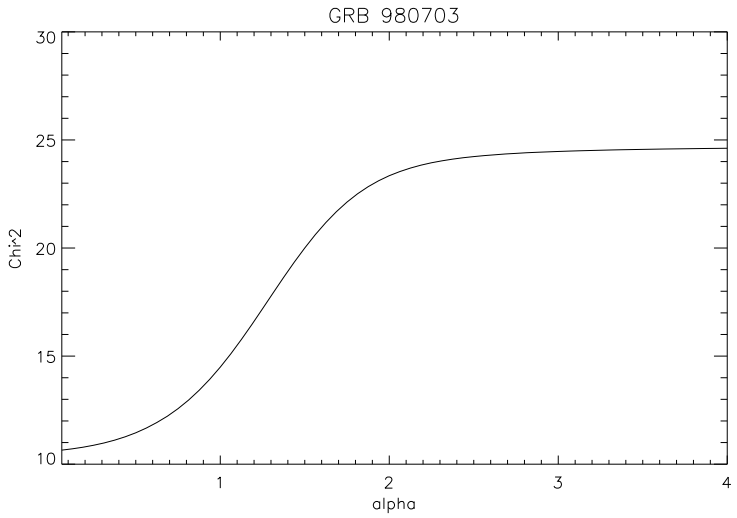

Figure 6.2: χ^2/dof as a function of index α (equation (6.1)) for GRB 980703. The best fit was achieved for the smallest α (starburst).

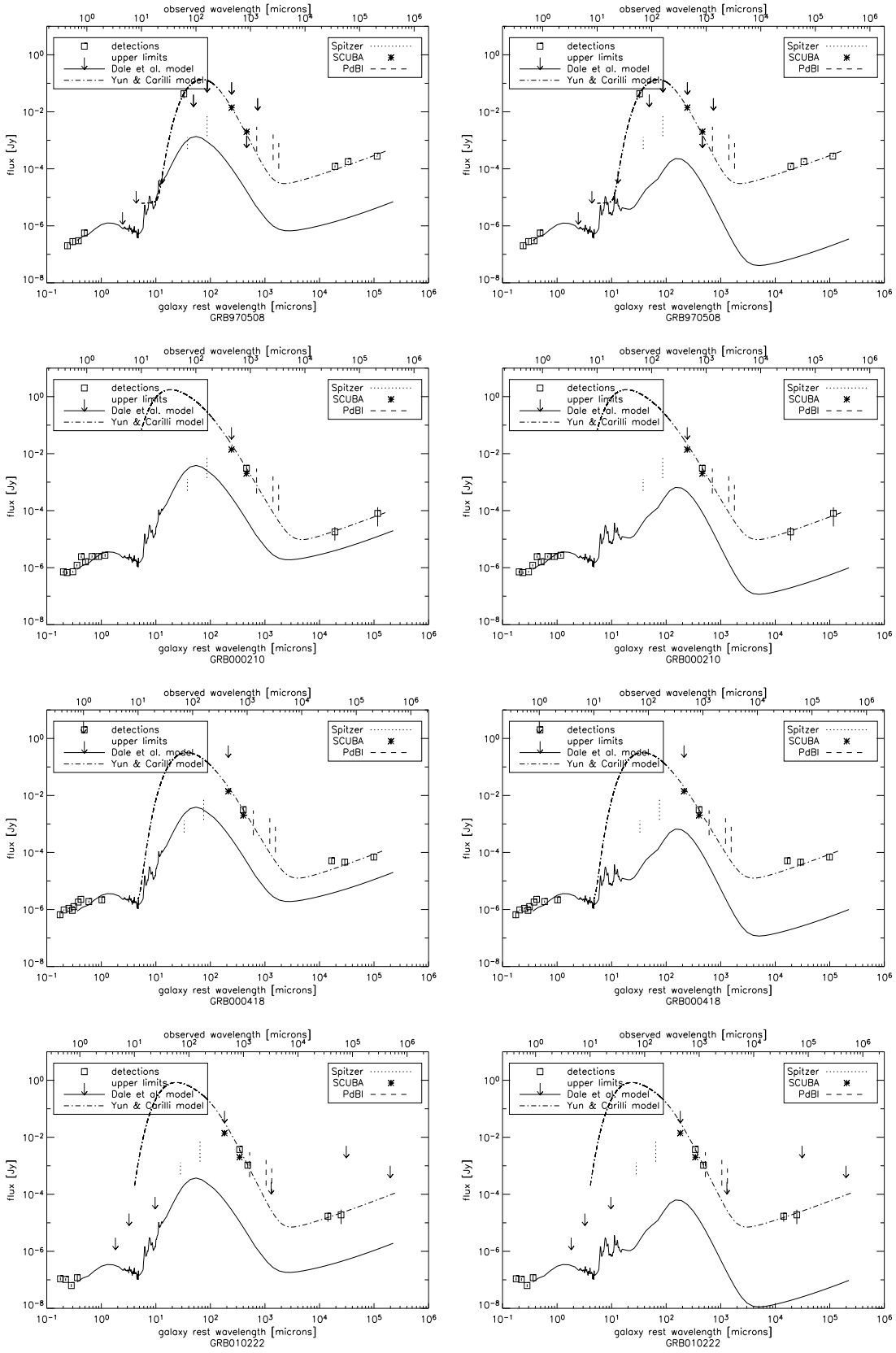

Figure 6.3: The model of Dale et al. (2001a) fitted to the optical / NIR (only) observations of GRB hosts. Left: $\alpha = 0.0625$, right: $\alpha = 4.0$ (equation (6.1)). (See insets for a description of the symbols.

Chapter 7

Empirical Model

7.1 Description

Having in mind that none of the existing SED models fitted well to the GRB host data, I constructed my own empirical model aiming at describing, reasonably well, both the short- and the long-wavelength parts of the spectrum. I used the GRASIL[1] software described by Silva et al. (1998).

GRASIL is a numerical code that calculates the spectrum of a galaxy by means of a radiative transfer method, applied to photons produced by a stellar population, and reprocessed by dust. The importance of this model is the fact that it is self-consistent, that it fulfills the principle of energy conservation between the energy absorbed by dust in the UV/optical wavelengths and the energy re-emitted in the infrared. Photons are influenced by dust, mostly for $\lambda \lesssim 1\,\mu$m (Silva et al. 1998) and the absorption is, on average, stronger for shorter wavelengths (e.g. Cardelli et al. 1989). However the density in molecular clouds (MCs) is so high that even IR photons are self-absorbed. Approximately 30% of the starlight is reprocessed by dust. This effect is especially important in galaxies with high star formation because of their high dust content. Hence, in the case of GRB hosts, it must be carefully implemented since they are claimed to have high SFRs (e.g. Tanvir et al. 2004).

The UV/optical/NIR emission of stars is summed up from the grid of simple stellar populations (SSPs)'integrated spectra. A SSP is a group of stars born at the same time and place, sharing the same age and metallicity, and with a particular type of IMF. The Salpeter (1955) IMF was used with $M_{\rm min} = 0.15 M_{\odot}$ and $M_{\rm max} = 120 M_{\odot}$. The evolution of each star depends on its mass and is tracked by evolutionary models. SSPs are taken from stellar

[1] `http://web.pd.astro.it/granato/grasil/grasil.html`

spectral libraries developed by Bertelli et al. (1994). They include stars with ages from 1 Myr to 20 Gyrs and metallicities $Z = 0.004$, 0.008, $0.02(= Z_{\odot})$, 0.05, 0.1.

Dust grains vary in size between 8 Å and 2 500 Å following a broken power-law distribution with an index of -3.5 for sizes above 50 Å and -4.0 for smaller grains. Grains bigger than 100 Å are assumed to be in thermal equilibrium with the radiating field, emitting a gray body spectrum, whereas smaller grains fluctuate in temperature. The photon absorption cross-section of PAHs depends on the wavelength and PAHs are responsible for emission/absorption features at 3.3, 6.2, 7.7, 8.6 and 11.3 μm.

A galaxy is an axially symmetric system. Free gas not incorporated into stars and dust are distributed throughout the galaxy in two forms: as diffuse medium and inside star-forming molecular clouds (MCs), as shown in Figure 7.1. New stars are born in MCs and then gradually escape from them. Hence the fraction f of SSP energy produced inside MCs at time t is:

$$f = \begin{cases} 1 & \text{if } t \leq t_0 \\ 2 - t/t_0 & \text{if } t_0 < t \leq 2t_0 \\ 0 & \text{if } t > 2t_0, \end{cases} \tag{7.1}$$

where t_0 is the model parameter indicating the time, after the starburst, when the first stars escape from MCs. The first epoch of star-forming activity is almost totally obscured in optical wavelengths because stars are formed in dense MCs and it takes time to escape from them.

The modelling involves calculating the history of SFR, the IMF, the metallicity and the residual gas fraction, from the time of the galaxy creation up to the age of the galaxy. Using this information the galaxy SED is built at the time of interest. In the case of a dust-free galaxy, spectra of all stars at this time are simply added. When dust is present radiation transfer is applied to calculate the attenuation.

Once the SED is obtained one can get additional information out. The SFR can be calculated from infrared emission (equation 6.2). The gray body curve (equation (5.4)) can be fitted to the region around the IR dust emission peak ($\sim 100\,\mu$m) and the dust temperature T_d and emissivity index β can be constrained. Then the dust mass can be estimated with equation (5.9).

7.2 Results and Discussion

7.2.1 Fitting Parameters

Figure 6.3 showed that submm and radio emissions were underestimated even for the most starbursting model of Dale et al. (2001a). Therefore the

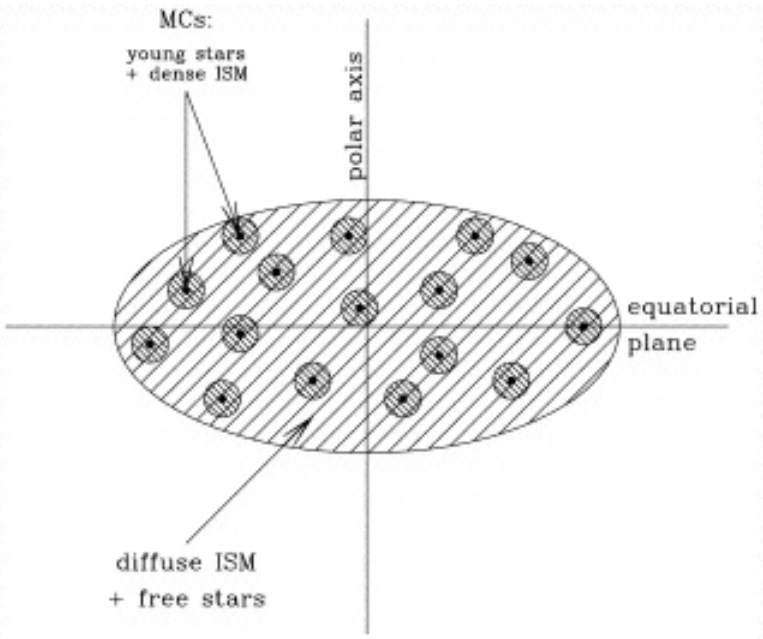

Figure 7.1: The distribution of stars and gas in the model of Silva et al. (1998).

starting point was to investigate how SEDs of dusty galaxies fitted the data. The fit for Arp 220, a nearby ULIRG (Ultra Luminous InfraRed Galaxy), is shown in Figure 7.2. Even in the case of this dusty star-forming galaxy, the long-wavelength emission of GRB hosts was underestimated. However, the discrepancy was not as big as before (Figure 6.3), so I used Arp 220 as a base of the SED modeling — I input the GRASIL parameters for this galaxy and varied them in order to match GRB hosts data.

At a first glance increasing of the amount of dust might appear to be successful, because in this way the submm emission is enhanced. However, Arp 220 is a red galaxy (has a steep flux decline in the optical domain for shorter wavelengths) and this change made it even redder. This was in contradiction with the blue colours (flat optical spectra) of GRB hosts (see Figure 7.2). The implemented solution was to construct SEDs assuming low ages for the galaxies. On one hand the majority of the stars still resides in dense molecular clouds, so a significant part of the energy is absorbed and re-emitted. This increases the dust emission. On the other hand there are lots of young, hot, blue stars in such a galaxy, because they have not finished their lives yet. Hence the total optical spectrum of the galaxy is blue.

The fact that GRBs reside in molecular clouds was confirmed by Galama

GRB host	t [Gyr]	dust/gas $[10^{-2}]$	$M_{\rm cloud}$ $[10^6 M_\odot]$	graphites / silicates	$M_{\rm burst}$ $[M_{\rm tot}]$
980703	2	0.3	0.9	9	0.03
000210	0.3	4	1	1	0.30
000418	0.14	1	1	1	0.05
010222	0.09	0.7	1	0.25	0.10
Arp 220	13	1	1	1	0.12

Table 7.1: GRASIL parameters yielding SEDs consistent with the data: age of the galaxy, dust-to-gas ratio, mass of the molecular clouds, ratio of abundances of graphite and silicate grains and mass of the burst in units of the total infalling mass of gas. The Arp 220 parameters are given for the comparison.

& Wijers (2001) who found that gas column densities derived from X-ray afterglows in a sample of 8 GRBs (including GRB 980703, discussed here) were in the range $10^{22}-10^{23}$ cm^{-2}, what corresponded to the column densities of giant molecular clouds in the Milky Way.

For each host I was able to construct an SED that fitted reasonably well to the data. A set of parameters is presented in Table 7.1. All the galaxies obtained were young ($t < 2$ Gyrs). The bigger the difference between optical and radio fluxes, the lower the age that was needed. This is because a younger galaxy has more stars still embedded in molecular clouds, so optical light is weaker and dust emission stronger. The ages for the hosts of GRB 000210 and GRB 000418 agreed, within a factor of 2, with the values derived by Christensen et al. (2004a). My estimation provided a very secure evidence of the low ages of some GRB hosts, based on all available data. This result is also consistent with the high dust temperatures derived in Section 5.4.3 (see discussion there).

The fraction of dust over gas was high, when compared with Arp 220, for only for one host (GRB 000210). This was expected in light of the previous discussion that the crucial parameter was not the amount of dust, but the age of the galaxy.

For one host (GRB 980703) I lowered slightly the mass of the molecular clouds and, in turn their optical depth, to achieve better consistency with the data.

I adjusted the ratio between graphite and silicate grains for GRB 980703 and GRB 010222. In the former case I needed more graphites in order to increase the absorption near the observed 8 μm band to be consistent with a *Spitzer* upper limit. In the latter case more silicates produced a deep

GRB host	SFR $[M_\odot/\mathrm{yr}]$	T_d [K]	β	M_d $[10^7 M_\odot]$	χ^2
980703	179	47	0.70	26	3.61
000210	138	63	1.44	13	1.27
000418	380	63	0.05	60	2.86
010222	366	51	1.14	31	2.34
Arp 220	580	56	1.32	30	-

Table 7.2: Characteristics of the galaxies derived from the SED modeling: star formation rate, temperature of dust, emissivity index, mass of dust and χ^2 of the fit. Values corresponding to Arp 220 are given for the comparison.

absorption feature below an observed 24 μm upper limit.

The burst was set to occur during the last 50 Myrs. Its mass was increased up to shift the radio part of the SED to match the data. It could be done because synchrotron radio emission is proportional to the SN rate (Bressan et al. 2002). If the mass of the burst is increased, a higher number of SNa implies more significant synchrotron radiation emitted by relativistic electrons accelerated in the shocked interstellar medium. Moreover small changes in the mass of the recent burst did not influence significantly other parts of the SED because the time scale of the burst was short. It affected only a number of relativistic electrons whose lifetimes are even shorter. Hence, radio emission is very sensitive to current SFR whereas IR emission depends on SFR averaged over the last a few tens Myrs what governs a number of massive stars.

7.2.2 Derived Values

Table 7.2 presents the parameters derived from the SEDs as explained in Section 7.1. SFRs were high (several hundreds $M_\odot/\mathrm{yr}$), yet lower than the values derived in Chapter 5 (see Table 5.2) by, approximately, a factor of 3. It revealed that there was a systematic difference in luminosity $\longrightarrow$ SFR scaling between the formalisms of Yun & Carilli (2002) and Silva et al. (1998). Such an uncertainty by a factor of a few uncertainty is common in the literature (see e.g. Buat & Xu 1996; Bressan et al. 2002). It accounts for the fact that the amount of energy re-emitted in the infrared is tied to newly born stars in very complicated ways that involve different densities, compositions, metallicities of the star forming regions, different stellar populations and many other factors such as the geometry of the star-forming clouds and the influence of surrounding stars and the gravitational potential of the galaxy

as a whole. Therefore different methods to estimate SFRs usually yield significantly different results.

The values of the temperature were also lower than those from the function of Yun & Carilli (2002). A more complete wavelength coverage of the SED in the dust emission domain would be necessary to judge which estimation is better. Especially, datapoints at wavelengths shorter than the peak (FIR) would be valuable. However, taking into account a scatter in submm-radio correlations (see Section 5.4.3), the values derived in this Chapter were similar to the temperature lower limits derived in Chapter 5. It indicated that these findings were consistent and that the difference was lower than the systematics such as the assumed submm-radio correlation.

As expected, dust masses were, within a factor of 2, consistent with the value for Arp 220. It placed the GRB hosts presented here in the dusty galaxies category. In Chapter 5 lower values were obtained. This was because temperatures in this Chapter were lower, so more dust needed to be present in the galaxies to explain their submm emission.

The goodness of the fit was reasonable. Although there were some individual outlying datapoints slightly inconsistent with the model at the level of $2-3\sigma$, it reproduced accurately the trends in SEDs.

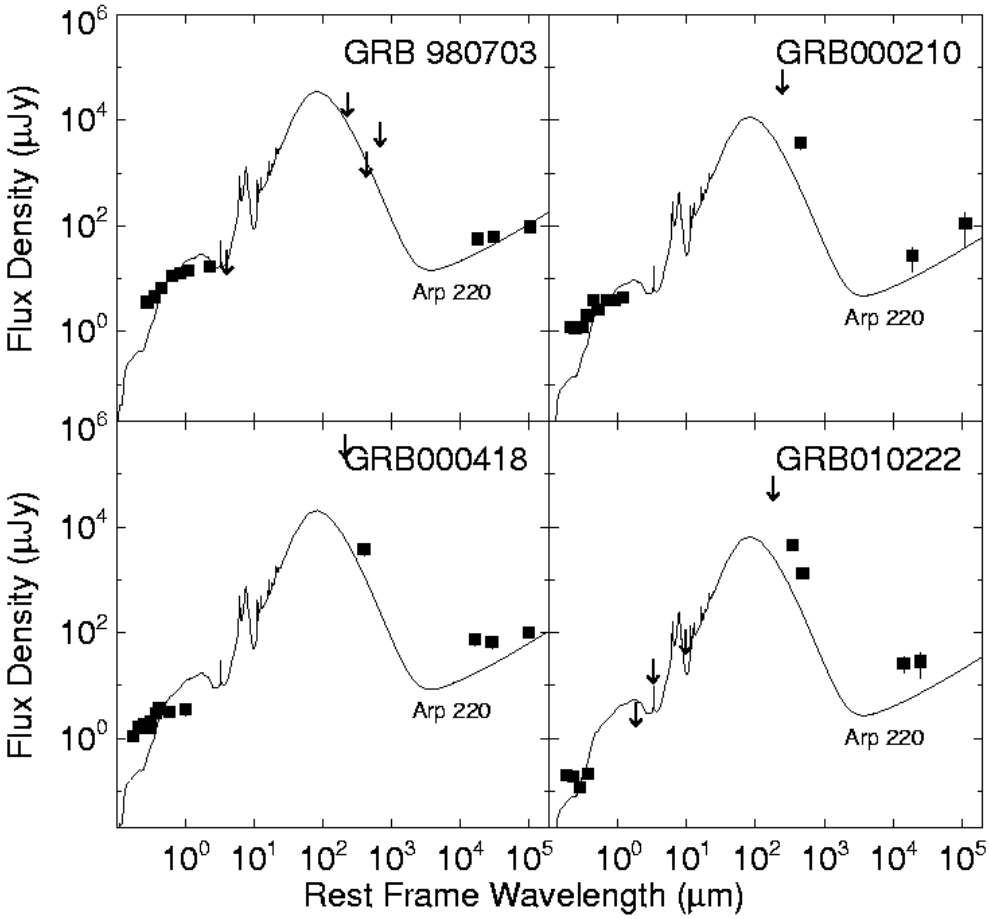

Figure 7.2: The Scaled Arp 220 model compared with SEDs of GRB hosts. A clear underestimation of long-wavelength emission is visible.

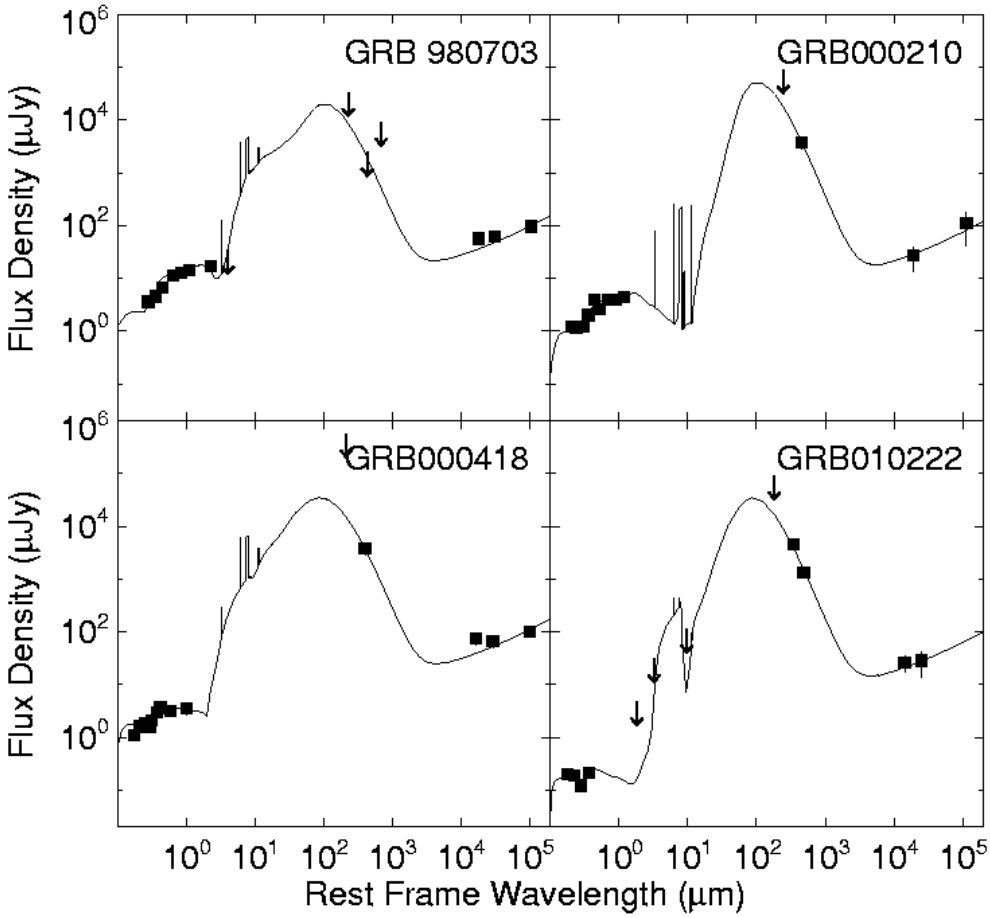

Figure 7.3: SEDs of GRB hosts calculated using GRASIL. The model is consistent with all the data.

Chapter 8

Summary

8.1 Conclusions

I presented the first successful fits of the entire optical to radio SED models to the existing photometric data of either submm or radio bright (detected) GRB host galaxies. The thesis deals for the most part with host properties at long wavelengths. These properties have not been explored in detail previously, although they give unobscured view on the host galaxies. This work gives the important constraints on GRB hosts in a new manner using all available data simultaneously.

The method proposed by Yun & Carilli (2002) seems to be accurate and powerful — it is well understood and analytical. Even for a few photometric points several galaxy characteristics of the host galaxies may be derived. I was able to confirm their high SFRs with greater confidence because they were based on several, not just one, photometric points. I placed lower limits on the host dust temperatures that were well above the average of submm, starburst and quiescent galaxies. This finding indicates, in a new and unique manner, that GRB hosts are young galaxies and is important in a still widely discussed context of the connection of GRBs with the star-formation. Although the determination of the temperature was based only on one submm datapoint and several non-thermal radio datapoints, the lower limits were robust and their reliance was investigated carefully.

I fitted different SED templates, ranging from quiescent to starburst galaxies, to the GRB host data. I discovered that no template matched all the available data in 3 out of 4 cases. Even starburst templates did not reproduce overall the SEDs, greatly underestimating the submm/radio emission and resulting in optical colors that were too red. This implied that the GRB hosts discussed here were not similar either to local starburst or submm

galaxies, but formed a separate class of galaxies.

My SED fittings utilised the GRASIL code and were successful for the entire optical to radio wavelength domain. Such fit had not been achieved before for any GRB host. These findings are important, since the understanding of a galaxy SED is crucial for having insight into the physical processes governing its emission. The templates derived matched the overall trends in energy distribution and allowed to constrain many parameters for these galaxies. Most importantly I securely confirmed that they were young galaxies with most of the star-formation embedded in molecular clouds and with high total star-formation rates. I was also able to explain enhanced submm/radio emission of hosts even though the galaxies were blue. Their low ages provide an explanation since young galaxies may emit in long-wavelengths and have blue color at the same time. These results indicate the connection between GRBs and star-formation, which can enable Star Formation History studies using GRBs.

The methods described here were applied in the context of GRB host galaxies at redshift $z \sim 1$ (Castro Cerón et al. 2006). Moreover the results for GRB hosts described here were presented by myself at the conference "The Multicoloured Landscape of Compact Objects and their Explosive Origins: Theory vs. Observations", Cefalù, Italy, and are going to be published in Michałowski et al. (2006).

8.2 Outlook

The research presented here will be continued by increasing the size of the sample of analysed hosts, as well as by building up the complexity of this analysis. One of possible future prospects is to concentrate on dust in GRB hosts — to compare the size distribution of grains (using e.g. formalism of Chen et al. 2006b) with the IR emission of these grains in order to constrain their properties.

Moreover, the fits should be investigated in the context of metallicity. It is important to establish if GRBs trace the metal-poor environments (see Section 3.1) and it is possible to address this issue in the SED fitting of their hosts. Additionally ages derived in this thesis should be checked against the age-metallicity degeneracy (Worthey 1994). This can not however change dramatically the conclusion of low ages of GRB hosts because, should the metallicity is lowered by 20%, the age should also be lowered (by 30%) to achieve a similar SED.

The lower limits on dust temperatures can be further checked by using different SED templates (e.g. those from Dale et al. 2001a), fitting them to

long-wavelength data and deriving the temperatures by a gray-body curve fitting. If one gets similar values, the estimations will seem more reliable.

In order to address the issue of specific SFRs of GRB hosts presented here, I am going to calculate their stellar masses in a way described by Castro Cerón et al. (2006) and compare the results to several samples of galaxies.

The fittings will be much more reliable and many uncertainty problems can be overcome with a better wavelength coverage in the observations of GRB hosts. Thus mm, FIR and MIR observations, using for example the Plateu de Bure Interferometer (mm) in Grenoble or the *Spitzer* telescope (IR), are highly desirable. It is also important to increase the sample of hosts with at least several detections at long wavelengths that can enable overall SED fitting.

Bibliography

Amati, L., Frontera, F., Vietri, M., in't Zand, J. J. M., Soffitta, P., Costa, E., Del Sordo, S., Pian, E., Piro, L., Antonelli, L. A., Fiume, D. D., Feroci, M., Gandolfi, G., Guidorzi, C., Heise, J., Kuulkers, E., Masetti, N., Montanari, E., Nicastro, L., Orlandini, M., & Palazzi, E. 2000, Science, 290, 953

Antonelli, L. A., Piro, L., Vietri, M., Costa, E., Soffitta, P., Feroci, M., Amati, L., Frontera, F., Pian, E., Zand, J. J. M. i., Heise, J., Kuulkers, E., Nicastro, L., Butler, R. C., Stella, L., & Perola, G. C. 2000, ApJ, 545, L39

Appleton, P. N., Fadda, D. T., Marleau, F. R., Frayer, D. T., Helou, G., Condon, J. J., Choi, P. I., Yan, L., Lacy, M., Wilson, G., Armus, L., Chapman, S. C., Fang, F., Heinrichson, I., Im, M., Jannuzi, B. T., Storrie-Lombardi, L. J., Shupe, D., Soifer, B. T., Squires, G., & Teplitz, H. I. 2004, ApJS, 154, 147

Archibald, E. N., Jenness, T., Holland, W. S., Coulson, I. M., Jessop, N. E., Stevens, J. A., Robson, E. I., Tilanus, R. P. J., Duncan, W. D., & Lightfoot, J. F. 2002, MNRAS, 336, 1

Band, D., Matteson, J., Ford, L., Schaefer, B., Palmer, D., Teegarden, B., Cline, T., Briggs, M., Paciesas, W., Pendleton, G., Fishman, G., Kouveliotou, C., Meegan, C., Wilson, R., & Lestrade, P. 1993, ApJ, 413, 281

Barnard, V. E., Blain, A. W., Tanvir, N. R., Natarajan, P., Smith, I. A., Wijers, R. A. M. J., Kouveliotou, C., Rol, E., Tilanus, R. P. J., & Vreeswijk, P. 2003, MNRAS, 338, 1

Berger, E. 2003, in AIP Conf. Proc.: Gamma-Ray Burst and Afterglow Astronomy 2001: A Workshop Celebrating the First Year of the HETE Mission, 662, ed. G. R. Ricker & R. K. Vanderspek, 420, `arXiv:astro-ph/0112559`

Berger, E., Cowie, L. L., Kulkarni, S. R., Frail, D. A., Aussel, H., & Barger, A. J. 2003, ApJ, 588, 99

Berger, E., Diercks, A., Frail, D. A., Kulkarni, S. R., Bloom, J. S., Sari, R., Halpern, J., Mirabal, N., Taylor, G. B., Hurley, K., Pooley, G., Becker, K. M., Wagner, R. M., Terndrup, D. M., Statler, T., Wik, D. R., Mazets, E., & Cline, T. 2001a, ApJ, 556, 556

Berger, E., Kulkarni, S. R., & Frail, D. A. 2001b, ApJ, 560, 652

Bertelli, G., Bressan, A., Chiosi, C., Fagotto, F., & Nasi, E. 1994, A&A Suppl., 106, 275

Bessell, M. S. 1979, PASP, 91, 589

Bessell, M. S. & Brett, J. M. 1988, PASP, 100, 1134

Blain, A. W., Chapman, S. C., Smail, I., & Ivison, R. 2004, ApJ, 611, 52

Blain, A. W., Ivison, R. J., & Smail, I. 1998, MNRAS, 296, L29

Blain, A. W., Jameson, A., Smail, I., Longair, M. S., Kneib, J.-P., & Ivison, R. J. 1999a, MNRAS, 309, 715

Blain, A. W. & Natarajan, P. 2000, MNRAS, 312, L35

Blain, A. W., Smail, I., Ivison, R. J., & Kneib, J.-P. 1999b, in ASP Conf. Ser. 193: The Hy-Redshift Universe: Galaxy Formation and Evolution at High Redshift, 425

Blain, A. W., Smail, I., Ivison, R. J., & Kneib, J.-P. 1999c, MNRAS, 302, 632

Bloom, J. S., Berger, E., Kulkarni, S. R., Djorgovski, S. G., & Frail, D. A. 2003, AJ, 125, 999

Bloom, J. S., Djorgovski, S. G., Kulkarni, S. R., & Frail, D. A. 1998, ApJ, 507, L25

Bloom, J. S., Kulkarni, S. R., & Djorgovski, S. G. 2002, AJ, 123, 1111

Bloom, J. S., Kulkarni, S. R., Djorgovski, S. G., Eichelberger, A. C., Cote, P., Blakeslee, J. P., Odewahn, S. C., Harrison, F. A., Frail, D. A., Filippenko, A. V., Leonard, D. C., Riess, A. G., Spinrad, H., Stern, D., Bunker, A., Dey, A., Grossan, B., Perlmutter, S., Knop, R. A., Hook, I. M., & Feroci, M. 1999a, Nat, 401, 453

Bloom, J. S., Sigurdsson, S., & Pols, O. R. 1999b, MNRAS, 305, 763

Bressan, A., Silva, L., & Granato, G. L. 2002, A&A, 392, 377

Briggs, M. S. 1995, Astrophys. Space Sci., 231, 3

Buat, V. & Xu, C. 1996, A&A, 306, 61

Bulik, T., Belczyński, K., & Zbijewski, W. 1999a, A&A Suppl., 138, 483

—. 1999b, MNRAS, 309, 629

Butler, N. R., Marshall, H. L., Ricker, G. R., Vanderspek, R. K., Ford, P. G., Crew, G. B., Lamb, D. Q., & Jernigan, J. G. 2003, ApJ, 597, 1010

Caputi, K. I., Dole, H., Lagache, G., McLure, R. J., Puget, J.-L., Rieke, G. H., Dunlop, J. S., Le Floc'h, E., Papovich, C., & Pérez-González, P. G. 2006, ApJ, 637, 727

Cardelli, J. A., Clayton, G. C., & Mathis, J. S. 1989, ApJ, 345, 245

Castro Cerón, J. M., Castro-Tirado, A. J., Gorosabel, J., Hjorth, J., Fynbo, J. U., Jensen, B. L., Pedersen, H., Andersen, M. I., López-Corredoira, M., Suárez, O., Grosdidier, Y., Casares, J., Pérez-Ramírez, D., Milvang-Jensen, B., Mallén-Ornelas, G., Fruchter, A., Greiner, J., Pian, E., Vreeswijk, P. M., Barthelmy, S. D., Cline, T., Frontera, F., Kaper, L., Klose, S., Kouveliotou, C., Hartmann, D. H., Hurley, K., Masetti, N., Mazets, E., Palazzi, E., Park, H. S., Rol, E., Salamanca, I., Tanvir, N., Trombka, J. I., Wijers, R. A. M. J., Williams, G. G., & van den Heuvel, E. 2002, A&A, 393, 445

Castro Cerón, J. M., Michałowski, M., Hjorth, J., Watson, D. J., Fynbo, J. P. U., & Gorosabel, J. 2006, ApJ, submitted

Castro-Tirado, A. J. & Gorosabel, J. 1999, A&A Suppl., 138, 449

Castro-Tirado, A. J., Zapatero-Osorio, M. R., Gorosabel, J., Greiner, J., Heidt, J., Herranz, D., Kemp, S. N., Martínez-González, E., Oscoz, A., Ortega, V., Röser, H.-J., Wolf, C., Pedersen, H., Jaunsen, A. O., Korhonen, H., Ilyin, I., Duemmler, R., Andersen, M. I., Hjorth, J., Henden, A. A., Vrba, F. J., Fried, J. W., Frontera, F., & Nicastro, L. 1999, ApJ, 511, L85

Cavallo, G. & Rees, M. J. 1978, MNRAS, 183, 359

Chapman, S. C., Blain, A. W., Ivison, R. J., & Smail, I. R. 2003, Nat, 422, 695

Chapman, S. C., Blain, A. W., Smail, I., & Ivison, R. J. 2005, ApJ, 622, 772

Chen, H.-W., Prochaska, J. X., & Bloom, J. S. 2006a, `ArXiv:astro-ph/0602144`

Chen, S., Li, A., & Wei, D. 2006b, `arXiv:astro-ph/0603222`

Cheng, K. S. & Lu, T. 2001, ChJAA, 1, 1

Chevalier, R. A. & Li, Z.-Y. 1999, ApJ, 520, L29

Christensen, L., Hjorth, J., & Gorosabel, J. 2004a, A&A, 425, 913

—. 2005, ApJ, 631, L29

Christensen, L., Hjorth, J., Gorosabel, J., Vreeswijk, P., Fruchter, A., Sahu, K., & Petro, L. 2004b, A&A, 413, 121

Condon, J. J. 1992, ARA&A, 30, 575

Conselice, C. J., Vreeswijk, P. M., Fruchter, A. S., Levan, A., Kouveliotou, C., Fynbo, J. P. U., Gorosabel, J., Tanvir, N. R., & Thorsett, S. E. 2005, ApJ, 633, 29

Costa, E., Frontera, F., Heise, J., Feroci, M., in 't Zand, J., Fiore, F., Cinti, M. N., dal Fiume, D., Nicastro, L., Orlandini, M., Palazzi, E., Rapisarda, M., Zavattini, G., Jager, R., Parmar, A., Owens, A., Molendi, S., Cusumano, G., Maccarone, M. C., Giarrusso, S., Coletta, A., Antonelli, L. A., Giommi, P., Muller, J. M., Piro, L., & Butler, R. C. 1997, Nat, 387, 783

Courty, S., Björnsson, G., & Gudmundsson, E. H. 2004, MNRAS, 354, 581

Dale, D. A. & Helou, G. 2002, ApJ, 576, 159

Dale, D. A., Helou, G., Contursi, A., Silbermann, N. A., & Kolhatkar, S. 2001a, ApJ, 549, 215

Dale, D. A., Helou, G., Neugebauer, G., Soifer, B. T., Frayer, D. T., & Condon, J. J. 2001b, AJ, 122, 1736

Djorgovski, S. G., Kulkarni, S. R., Bloom, J. S., Frail, D. A., Harrison, F. A., Galama, T. J., Reichart, D., Castro, S. M., Fox, D., Sari, R., Berger, E., Price, P., Yost, S., Goodrich, R., & Chaffee, F. 2001, in Gamma-ray Bursts in the Afterglow Era, ed. E. Costa, F. Frontera, & J. Hjorth, 218

Djorgovski, S. G., Kulkarni, S. R., Bloom, J. S., Goodrich, R., Frail, D. A., Piro, L., & Palazzi, E. 1998, ApJ, 508, L17

Dunne, L. & Eales, S. A. 2001, MNRAS, 327, 697

Economou, F., Bridger, A., Wright, G. S., Jenness, T., Currie, M. J., & Adamson, A. 1999, in ASP Conf. Ser. 172: Astronomical Data Analysis Software and Systems VIII, 11

Fargion, D. 2001, in Gamma-ray Bursts in the Afterglow Era, ed. E. Costa, F. Frontera, & J. Hjorth, 315

Fenimore, E. E., Epstein, R. I., Ho, C., Klebesadel, R. W., Lacey, C., Laros, J. G., Meier, M., Strohmayer, T., Pendleton, G., Fishman, G., Kouveliotou, C., & Meegan, C. 1993, Nat, 366, 40

Filippenko, A. V. 1997, ARA&A, 35, 309

Fishman, G. J. & Meegan, C. A. 1995, ARA&A, 33, 415

Frail, D. A., Bertoldi, F., Moriarty-Schieven, G. H., Berger, E., Price, P. A., Bloom, J. S., Sari, R., Kulkarni, S. R., Gerardy, C. L., Reichart, D. E., Djorgovski, S. G., Galama, T. J., Harrison, F. A., Walter, F., Shepherd, D. S., Halpern, J., Peck, A. B., Menten, K. M., Yost, S. A., & Fox, D. W. 2002, ApJ, 565, 829

Frail, D. A., Kulkarni, S. R., Nicastro, S. R., Feroci, M., & Taylor, G. B. 1997, Nat, 389, 261

Frail, D. A., Waxman, E., & Kulkarni, S. R. 2000, ApJ, 537, 191

Fruchter, A., Krolik, J. H., & Rhoads, J. E. 2001, ApJ, 563, 597

Fruchter, A. S., Levan, A. J., Strolger, L., Vreeswijk, P. M., Thorsett, S. E., Bersier, D., Burud, I., Castro Cerón, J. M., Castro-Tirado, A. J., Conselice, C., Dahlen, T., Ferguson, H. C., Fynbo, J. P. U., Garnavich, P. M., Gibbons, R. A., Gorosabel, J., Gull, T. R., Hjorth, J., Holland, S. T., Kouveliotou, C., Levay, Z., Livio, M., Metzger, M. R., Nugent, P. E., Petro, L., Pian, E., Rhoads, J. E., Riess, A. G., Sahu, K. C., Smette, A., Tanvir, N. R., Wijers, R. A. M. J., & Woosley, S. E. 2006, Nat, 441, 463

Fruchter, A. S., Pian, E., Thorsett, S. E., Bergeron, L. E., González, R. A., Metzger, M., Goudfrooij, P., Sahu, K. C., Ferguson, H., Livio, M., Mutchler, M., Petro, L., Frontera, F., Galama, T., Groot, P., Hook, R., Kouveliotou, C., Macchetto, D., van Paradijs, J., Palazzi, E., Pedersen, H., Sparks, W., & Tavani, M. 1999a, ApJ, 516, 683

Fruchter, A. S., Thorsett, S. E., Metzger, M. R., Sahu, K. C., Petro, L., Livio, M., Ferguson, H., Pian, E., Hogg, D. W., Galama, T., Gull, T. R., Kouveliotou, C., Macchetto, D., van Paradijs, J., Pedersen, H., & Smette, A. 1999b, ApJ, 519, L13

Fynbo, J. P. U., Jakobsson, P., Möller, P., Hjorth, J., Thomsen, B., Andersen, M. I., Fruchter, A. S., Gorosabel, J., Holland, S. T., Ledoux, C., Pedersen, H., Rhoads, J., Weidinger, M., & Wijers, R. A. M. J. 2003, A&A, 406, L63

Fynbo, J. U., Holland, S., Andersen, M. I., Thomsen, B., Hjorth, J., Björnsson, G., Jaunsen, A. O., Natarajan, P., & Tanvir, N. 2000, ApJ, 542, L89

Galama, T. J., Reichart, D., Brown, T. M., Kimble, R. A., Price, P. A., Berger, E., Frail, D. A., Kulkarni, S. R., Yost, S. A., Gal-Yam, A., Bloom, J. S., Harrison, F. A., Sari, R., Fox, D., & Djorgovski, S. G. 2003, ApJ, 587, 135

Galama, T. J., Vreeswijk, P. M., van Paradijs, J., Kouveliotou, C., Augusteijn, T., Bohnhardt, H., Brewer, J. P., Doublier, V., Gonzalez, J.-F., Leibundgut, B., Lidman, C., Hainaut, O. R., Patat, F., Heise, J., in 't Zand, J., Hurley, K., Groot, P. J., Strom, R. G., Mazzali, P. A., Iwamoto, K., Nomoto, K., Umeda, H., Nakamura, T., Young, T. R., Suzuki, T., Shigeyama, T., Koshut, T., Kippen, M., Robinson, C., de Wildt, P., Wijers, R. A. M. J., Tanvir, N., Greiner, J., Pian, E., Palazzi, E., Frontera, F., Masetti, N., Nicastro, L., Feroci, M., Costa, E., Piro, L., Peterson, B. A., Tinney, C., Boyle, B., Cannon, R., Stathakis, R., Sadler, E., Begam, M. C., & Ianna, P. 1998, Nat, 395, 670

Galama, T. J. & Wijers, R. A. M. J. 2001, ApJ, 549, L209

Garrett, M. A. 2002, A&A, 384, L19

Ghisellini, G. 2001, `arXiv:astro-ph/0111584`

Gillmon, K., Shull, J. M., Tumlinson, J., & Danforth, C. 2006, ApJ, 636, 891

Goodman, J. 1986, ApJ, 308, L47

Gorosabel, J., Christensen, L., Hjorth, J., Fynbo, J. U., Pedersen, H., Jensen, B. L., Andersen, M. I., Lund, N., Jaunsen, A. O., Castro Cerón, J. M., Castro-Tirado, A. J., Fruchter, A., Greiner, J., Pian, E., Vreeswijk, P. M., Burud, I., Frontera, F., Kaper, L., Klose, S., Kouveliotou, C., Masetti, N., Palazzi, E., Rhoads, J., Rol, E., Salamanca, I., Tanvir, N., Wijers, R. A. M. J., & van den Heuvel, E. 2003a, A&A, 400, 127

Gorosabel, J., Klose, S., Christensen, L., Fynbo, J. P. U., Hjorth, J., Greiner, J., Tanvir, N., Jensen, B. L., Pedersen, H., Holland, S. T., Lund, N., Jaunsen, A. O., Castro Cerón, J. M., Castro-Tirado, A. J., Fruchter, A., Pian, E., Vreeswijk, P. M., Burud, I., Frontera, F., Kaper, L., Kouveliotou, C., Masetti, N., Palazzi, E., Rhoads, J., Rol, E., Salamanca, I., Wijers, R. A. M. J., & van den Heuvel, E. 2003b, A&A, 409, 123

Gorosabel, J., Pérez-Ramírez, D., Sollerman, J., de Ugarte Postigo, A., Fynbo, J. P. U., Castro-Tirado, A. J., Jakobsson, P., Christensen, L., Hjorth, J., Jóhannesson, G., Guziy, S., Castro Cerón, J. M., Björnsson, G., Sokolov, V. V., Fatkhullin, T. A., & Nilsson, K. 2005, A&A, 444, 711

Granot, J. 2003, ApJ, 596, L17

Greiner, J. 1999, Memorie della Societa Astronomica Italiana, 70, 891

Haarsma, D. B., Partridge, R. B., Windhorst, R. A., & Richards, E. A. 2000, ApJ, 544, 641

Hanlon, L., Laureijs, R. J., Metcalfe, L., McBreen, B., Altieri, B., Castro-Tirado, A., Claret, A., Costa, E., Delaney, M., Feroci, M., Frontera, F., Galama, T., Gorosabel, J., Groot, P., Heise, J., Kessler, M., Kouveliotou, C., Palazzi, E., van Paradijs, J., Piro, L., & Smith, N. 2000, A&A, 359, 941

Helou, G. & Bicay, M. D. 1993, ApJ, 415, 93

Hildebrand, R. H. 1983, QJRAS, 24, 267

Hirashita, H., Hunt, L. K., & Ferrara, A. 2002, MNRAS, 330, L19

Hjorth, J., Holland, S., Courbin, F., Dar, A., Olsen, L. F., & Scodeggio, M. 2000, ApJ, 534, L147

Hjorth, J., Møller, P., Gorosabel, J., Fynbo, J. P. U., Toft, S., Jaunsen, A. O., Kaas, A. A., Pursimo, T., Torii, K., Kato, T., Yamaoka, H., Yoshida, A., Thomsen, B., Andersen, M. I., Burud, I., Castro Cerón, J. M., Castro-Tirado, A. J., Fruchter, A. S., Kaper, L., Kouveliotou, C., Masetti, N., Palazzi, E., Pedersen, H., Pian, E., Rhoads, J., Rol, E., Tanvir, N. R., Vreeswijk, P. M., Wijers, R. A. M. J., & van den Heuvel, E. P. J. 2003a, ApJ, 597, 699

Hjorth, J., Pedersen, H., Jaunsen, A. O., & Andersen, M. I. 1999, A&A Suppl., 138, 461

Hjorth, J., Pian, E., & Fynbo, J. P. U. 2004, Nuclear Physics B Proceedings Supplements, 132, 271

Hjorth, J., Sollerman, J., Møller, P., Fynbo, J. P. U., Woosley, S. E., Kouveliotou, C., Tanvir, N. R., Greiner, J., Andersen, M. I., Castro-Tirado, A. J., Castro Cerón, J. M., Fruchter, A. S., Gorosabel, J., Jakobsson, P., Kaper, L., Klose, S., Masetti, N., Pedersen, H., Pedersen, K., Pian, E., Palazzi, E., Rhoads, J. E., Rol, E., van den Heuvel, E. P. J., Vreeswijk, P. M., Watson, D., & Wijers, R. A. M. J. 2003b, Nat, 423, 847

Hjorth, J., Thomsen, B., Nielsen, S. R., Andersen, M. I., Holland, S. T., Fynbo, J. U., Pedersen, H., Jaunsen, A. O., Halpern, J. P., Fesen, R., Gorosabel, J., Castro-Tirado, A., McMahon, R. G., Hoenig, M. D., Björnsson, G., Amati, L., Tanvir, N. R., & Natarajan, P. 2002, ApJ, 576, 113

Hogg, D. W., Baldry, I. K., Blanton, M. R., & Eisenstein, D. J. 2002, `arXiv:astro-ph/0210394`

Hogg, D. W. & Fruchter, A. S. 1999, ApJ, 520, 54

Holland, S. 2001, in AIP Conf. Proc. 586: 20th Texas Symposium on relativistic astrophysics, ed. J. C. Wheeler & H. Martel, 593

Holland, S., Fynbo, J. P. U., Hjorth, J., Gorosabel, J., Pedersen, H., Andersen, M. I., Dar, A., Thomsen, B., Møller, P., Björnsson, G., Jaunsen, A. O., Natarajan, P., & Tanvir, N. 2001, A&A, 371, 52

Holland, S. & Hjorth, J. 1999, A&A, 344, L67

Holland, W. S., Robson, E. I., Gear, W. K., Cunningham, C. R., Lightfoot, J. F., Jenness, T., Ivison, R. J., Stevens, J. A., Ade, P. A. R., Griffin, M. J., Duncan, W. D., Murphy, J. A., & Naylor, D. A. 1999, MNRAS, 303, 659

Hurley, K., Kargatis, V., Liang, E., Barat, C., Eveno, E., Niel, M., Dolidze, V. S., Kozlenkov, A. A., Mitrofanov, I. G., & Pozanenko, A. S. 1992, in American Institute of Physics Conference Series, ed. W. S. Paciesas & G. J. Fishman, 195–200

Jakobsson, P., Björnsson, G., Fynbo, J. P. U., Jóhannesson, G., Hjorth, J., Thomsen, B., Møller, P., Watson, D., Jensen, B. L., Östlin, G., Gorosabel, J., & Gudmundsson, E. H. 2005, MNRAS, 362, 245

Jakobsson, P., Levan, A., Fynbo, J. P. U., Priddey, R., Hjorth, J., Tanvir, N., Watson, D., Jensen, B. L., Sollerman, J., Natarajan, P., Gorosabel, J., Castro Cerón, J. M., Pedersen, K., Pursimo, T., Árnadóttir, A. S., Castro-Tirado, A. J., Davis, C. J., Deeg, H. J., Fiuza, D. A., Mykolaitis, S., & Sousa, S. G. 2006, A&A, 447, 897

Jenness, T. & Economou, F. 1999, in ASP Conf. Ser. 172: Astronomical Data Analysis Software and Systems VIII, 171

Jenness, T. & Lightfoot, J. F. 1998, in ASP Conf. Ser. 145: Astronomical Data Analysis Software and Systems VII, 216

Jenness, T., Stevens, J. A., Archibald, E. N., Economou, F., Jessop, N. E., & Robson, E. I. 2002, MNRAS, 336, 14

Jensen, B. L. 2004, Master's thesis, University of Copenhagen

Kann, D. A., Klose, S., & Zeh, A. 2006, ApJ, 641, 993

Kennicutt, R. C. 1998, ARA&A, 36, 189

Klaas, U., Haas, M., Müller, S. A. H., Chini, R., Schulz, B., Coulson, I., Hippelein, H., Wilke, K., Albrecht, M., & Lemke, D. 2001, A&A, 379, 823

Klebesadel, R. W., Strong, I. B., & Olson, R. A. 1973, ApJ, 182, L85

Kommers, J. M., Lewin, W. H. G., Kouveliotou, C., van Paradijs, J., Pendleton, G. N., Meegan, C. A., & Fishman, G. J. 2000, ApJ, 533, 696

Kouveliotou, C., Koshut, T., Briggs, M., Pendleton, G., Meegan, C., Fishman, G., & Lestrade, J. 1995, Bulletin of the American Astronomical Society, 28, 759

Kouveliotou, C., Meegan, C. A., Fishman, G. J., Bhat, N. P., Briggs, M. S., Koshut, T. M., Paciesas, W. S., & Pendleton, G. N. 1993, ApJ, 413, L101

Kulkarni, S. R., Djorgoski, S. G., Ramaprakash, A. N., Goodrich, R., Bloom, J. S., Adelberger, K. L., Kundic, T., Lubin, L., Frail, D. A., Frontera, F., Feroci, M., Nicastro, L., Barth, A. J., Davis, M., Filippenko, A. V., & Newman, J. 1998a, Nat, 393, 35

Kulkarni, S. R., Frail, D. A., Wieringa, M. H., Ekers, R. D., Sadler, E. M., Wark, R. M., Higdon, J. L., Phinney, E. S., & Bloom, J. S. 1998b, Nat, 395, 663

Lamb, D. Q. & Reichart, D. E. 2000, ApJ, 536, 1

Le Floc'h, E., Charmandaris, V., Forrest, W. J., Mirabel, I. F., Armus, L., & Devost, D. 2006, ApJ, 642, 636

Le Floc'h, E., Duc, P.-A., Mirabel, I. F., Sanders, D. B., Bosch, G., Diaz, R. J., Donzelli, C. J., Rodrigues, I., Courvoisier, T. J.-L., Greiner, J., Mereghetti, S., Melnick, J., Maza, J., & Minniti, D. 2003, A&A, 400, 499

Levan, A., Fruchter, A., Rhoads, J., Mobasher, B., Tanvir, N., Gorosabel, J., Rol, E., Kouveliotou, C., Dell'Antonio, I., Merrill, M., Bergeron, E., Castro Cerón, J. M., Masetti, N., Vreeswijk, P., Antonelli, A., Bersier, D., Castro-Tirado, A., Fynbo, J., Garnavich, P., Holland, S., Hjorth, J., Nugent, P., Pian, E., Smette, A., Thomsen, B., Thorsett, S., & Wijers, R. 2006, `ArXiv:astro-ph/0608166`

Lilly, S. J., Tresse, L., Hammer, F., Crampton, D., & Le Fevre, O. 1995, ApJ, 455, 108

MacFadyen, A. I. & Woosley, S. E. 1999, ApJ, 524, 262

Madau, P., Ferguson, H. C., Dickinson, M. E., Giavalisco, M., Steidel, C. C., & Fruchter, A. 1996, MNRAS, 283, 1388

Madau, P., Pozzetti, L., & Dickinson, M. 1998, ApJ, 498, 106

Mao, S. & Mo, H. J. 1998, A&A, 339, L1

Meegan, C. A., Fishman, G. J., Wilson, R. B., Horack, J. M., Brock, M. N., Paciesas, W. S., Pendleton, G. N., & Kouveliotou, C. 1992, Nat, 355, 143

Meszaros, P. & Rees, M. J. 1997, ApJ, 476, 232

Metzger, M. R., Djorgovski, S. G., Kulkarni, S. R., Steidel, C. C., Adelberger, K. L., Frail, D. A., Costa, E., & Frontera, F. 1997, Nat, 387, 879

Michałowski, M., Hjorth, J., Castro Cerón, J. M., & Darach, W. 2006, American Institute of Physics, Proceedings of the Cefalù Conference, in preparation

Mirabal, N., Halpern, J. P., Chornock, R., Filippenko, A. V., Terndrup, D. M., Armstrong, E., Kemp, J., Thorstensen, J. R., Tavarez, M., & Espaillat, C. 2003, ApJ, 595, 935

Mirabel, F., Sanders, D. B., & Le Floc'h, E. 2000, in ASP Conf. Ser. 215: Cosmic Evolution and Galaxy Formation: Structure, Interactions, and Feedback, ed. J. Franco, L. Terlevich, O. López-Cruz, & I. Aretxaga, 192

Narayan, R., Piran, T., & Kumar, P. 2001, ApJ, 557, 949

Nemiroff, R. J. 1994, in AIP Conf. Proc. 307: Gamma-Ray Bursts, ed. G. J. Fishman, 730

Nomoto, K., Yamaoka, H., Pols, O. R., van den Heuvel, E. P. J., Iwamoto, K., Kumagai, S., & Shigeyama, T. 1994, Nat, 371, 227

Paczyński, B. 1986, ApJ, 308, L43

—. 1991, Acta Astronomica, 41, 257

—. 1995, PASP, 107, 1167

—. 1998, ApJ, 494, L45

Panaitescu, A. & Kumar, P. 2002, ApJ, 571, 779

Pérez-González, P. G., Rieke, G. H., Egami, E., Alonso-Herrero, A., Dole, H., Papovich, C., Blaylock, M., Jones, J., Rieke, M., Rigby, J., Barmby, P., Fazio, G. G., Huang, J., & Martin, C. 2005, ApJ, 630, 82

Pian, E., Fruchter, A. S., Bergeron, L. E., Thorsett, S. E., Frontera, F., Tavani, M., Costa, E., Feroci, M., Halpern, J., Lucas, R. A., Nicastro, L., Palazzi, E., Piro, L., Sparks, W., Castro-Tirado, A. J., Gull, T., Hurley, K., & Pedersen, H. 1998, ApJ, 492, L103

Piran, T. 1999, Phys. Rep., 314, 575

Piran, T. 2001, `arXiv:astro-ph/0104134`

Piran, T. 2005, Reviews of Modern Physics, 76, 1143

Piro, L., Costa, E., Feroci, M., Frontera, F., Amati, L., dal Fiume, D., Antonelli, L. A., Heise, J., in 't Zand, J., Owens, A., Parmar, A. N., Cusumano, G., Vietri, M., & Perola, G. C. 1999, ApJ, 514, L73

Piro, L., Frail, D. A., Gorosabel, J., Garmire, G., Soffitta, P., Amati, L., Andersen, M. I., Antonelli, L. A., Berger, E., Frontera, F., Fynbo, J., Gandolfi, G., Garcia, M. R., Hjorth, J., Zand, J. i., Jensen, B. L., Masetti, N., Møller, P., Pedersen, H., Pian, E., & Wieringa, M. H. 2002, ApJ, 577, 680

Piro, L., Garmire, G., Garcia, M., Stratta, G., Costa, E., Feroci, M., Mészáros, P., Vietri, M., Bradt, H., Frail, D., Frontera, F., Halpern, J., Heise, J., Hurley, K., Kawai, N., Kippen, R. M., Marshall, F., Murakami, T., Sokolov, V. V., Takeshima, T., & Yoshida, A. 2000, Science, 290, 955

Poirier, J., D'Andrea, C., Fragile, P. C., Gress, J., Mathews, G. J., & Race, D. 2003, Phys. Rev. D, 67, 042001

Priddey, R. S., Tanvir, N. R., Levan, A. J., Fruchter, A. S., Kouveliotou, C., Smith, I. A., & Wijers, R. A. M. J. 2006, `arXiv:astro-ph/0604463`

Prochaska, J. X., Bloom, J. S., Chen, H.-W., Hurley, K. C., Melbourne, J., Dressler, A., Graham, J. R., Osip, D. J., & Vacca, W. D. 2004, ApJ, 611, 200

Ramirez-Ruiz, E., Trentham, N., & Blain, A. W. 2002, MNRAS, 329, 465

Rees, M. J. & Meszaros, P. 1992, MNRAS, 258, 41P

Reeves, J. N., Watson, D., Osborne, J. P., Pounds, K. A., & O'Brien, P. T. 2003, A&A, 403, 463

Sagar, R., Stalin, C. S., Bhattacharya, D., Pandey, S. B., Mohan, V., Castro-Tirado, A. J., Pramesh Rao, A., Trushkin, S. A., Nizhelskij, N. A., Bremer, M., & Castro Cerón, J. M. 2001, Bulletin of the Astronomical Society of India, 29, 91

Sahu, K. C., Livio, M., Petro, L., Macchetto, F. D., van Paradijs, J., Kouveliotou, C., Fishman, G. J., Meegan, C. A., Groot, P. J., & Galama, T. 1997, Nat, 387, 476

Salpeter, E. E. 1955, ApJ, 121, 161

Sari, R., Piran, T., & Halpern, J. P. 1999, ApJ, 519, L17

Sari, R., Piran, T., & Narayan, R. 1998, ApJ, 497, L17

Savaglio, S., Fall, S. M., & Fiore, F. 2003, ApJ, 585, 638

Savaglio, S., Glazebrook, K., & Le Borgne, D. 2006, in AIP Conf. Proc. 838: Gamma-Ray Bursts in the Swift Era, ed. S. S. Holt, N. Gehrels, & J. A. Nousek, 540–545

Schaefer, B. E., Gerardy, C. L., Höflich, P., Panaitescu, A., Quimby, R., Mader, J., Hill, G. J., Kumar, P., Wheeler, J. C., Eracleous, M., Sigurdsson, S., Mészáros, P., Zhang, B., Wang, L., Hessman, F. V., & Petrosian, V. 2003, ApJ, 588, 387

Scott, S. E., Fox, M. J., Dunlop, J. S., Serjeant, S., Peacock, J. A., Ivison, R. J., Oliver, S., Mann, R. G., Lawrence, A., Efstathiou, A., Rowan-Robinson, M., Hughes, D. H., Archibald, E. N., Blain, A., & Longair, M. 2002, MNRAS, 331, 817

Scoville, N. Z., Sargent, A. I., Sanders, D. B., & Soifer, B. T. 1991, ApJ, 366, L5

Silva, L., Granato, G. L., Bressan, A., & Danese, L. 1998, ApJ, 509, 103

Smith, I. A., Tilanus, R. P. J., Tanvir, N., Barnard, V. E., Moriarty-Schieven, G. H., Frail, D. A., Wijers, R. A. M. J., Vreeswijk, P., Rol, E., & Kouveliotou, C. 2005, A&A, 439, 987

Smith, I. A., Tilanus, R. P. J., van Paradijs, J., Galama, T. J., Groot, P. J., Vreeswijk, P., Kouveliotou, C., Wijers, R. A. M. J., & Tanvir, N. 1999, A&A, 347, 92

Sokolov, V. V., Fatkhullin, T. A., Castro-Tirado, A. J., Fruchter, A. S., Komarova, V. N., Kasimova, E. R., Dodonov, S. N., Afanasiev, V. L., & Moiseev, A. V. 2001, A&A, 372, 438

Sollerman, J., Östlin, G., Fynbo, J. P. U., Hjorth, J., Fruchter, A., & Pedersen, K. 2005, New Astronomy, 11, 103

Solomon, P. M., Downes, D., Radford, S. J. E., & Barrett, J. W. 1997, ApJ, 478, 144

Stanek, K. Z., Gnedin, O. Y., Beacom, J. F., Gould, A. P., Johnson, J. A., Kollmeier, J. A., Modjaz, M., Pinsonneault, M. H., Pogge, R., & Weinberg, D. H. 2006, arXiv:astro-ph/0604113

Stanek, K. Z., Matheson, T., Garnavich, P. M., Martini, P., Berlind, P., Caldwell, N., Challis, P., Brown, W. R., Schild, R., Krisciunas, K., Calkins, M. L., Lee, J. C., Hathi, N., Jansen, R. A., Windhorst, R., Echevarria, L., Eisenstein, D. J., Pindor, B., Olszewski, E. W., Harding, P., Holland, S. T., & Bersier, D. 2003, ApJ, 591, L17

Stratta, G., Fiore, F., Antonelli, L. A., Piro, L., & De Pasquale, M. 2004, ApJ, 608, 846

Tagliaferri, G., Antonelli, L. A., Chincarini, G., Fernández-Soto, A., Malesani, D., Della Valle, M., D'Avanzo, P., Grazian, A., Testa, V., Campana, S., Covino, S., Fiore, F., Stella, L., Castro-Tirado, A. J., Gorosabel, J., Burrows, D. N., Capalbi, M., Cusumano, G., Conciatore, M. L., D'Elia, V., Filliatre, P., Fugazza, D., Gehrels, N., Goldoni, P., Guetta, D., Guziy, S., Held, E. V., Hurley, K., Israel, G. L., Jelínek, M., Lazzati, D., López-Echarri, A., Melandri, A., Mirabel, I. F., Moles, M., Moretti, A., Mason, K. O., Nousek, J., Osborne, J., Pellizza, L. J., Perna, R., Piranomonte, S., Piro, L., de Ugarte Postigo, A., & Romano, P. 2005, A&A, 443, L1

Tanvir, N. R., Barnard, V. E., Blain, A. W., Fruchter, A. S., Kouveliotou, C., Natarajan, P., Ramirez-Ruiz, E., Rol, E., Smith, I. A., Tilanus, R. P. J., & Wijers, R. A. M. J. 2004, MNRAS, 352, 1073

Taylor, E. L., Mann, R. G., Efstathiou, A. N., Babbedge, T. S. R., Rowan-Robinson, M., Lagache, G., Lawrence, A., Mei, S., Vaccari, M., Héraudeau, P., Oliver, S. J., Dennefeld, M., Perez-Fournon, I., Serjeant, S., González-Solares, E., Puget, J.-L., Dole, H., & Lari, C. 2005, MNRAS, 361, 1352

Totani, T. 1997, ApJ, 486, L71

Totani, T. & Takeuchi, T. T. 2002, ApJ, 570, 470

Trentham, N., Ramirez-Ruiz, E., & Blain, A. W. 2002, MNRAS, 334, 983

van der Kruit, P. C. 1973, A&A, 29, 263

van Paradijs, J., Groot, P. J., Galama, T., Kouveliotou, C., Strom, R. G., Telting, J., Rutten, R. G. M., Fishman, G. J., Meegan, C. A., Pettini, M., Tanvir, N., Bloom, J., Pedersen, H., Nordgaard-Nielsen, H. U., Linden-Vornle, M., Melnick, J., van der Steene, G., Bremer, M., Naber, R., Heise, J., in 't Zand, J., Costa, E., Feroci, M., Piro, L., Frontera, F., Zavattini, G., Nicastro, L., Palazzi, E., Bennet, K., Hanlon, L., & Parmar, A. 1997, Nat, 386, 686

Vreeswijk, P. M., Fruchter, A., Kaper, L., Rol, E., Galama, T. J., van Paradijs, J., Kouveliotou, C., Wijers, R. A. M. J., Pian, E., Palazzi, E., Masetti, N., Frontera, F., Savaglio, S., Reinsch, K., Hessman, F. V., Beuermann, K., Nicklas, H., & van den Heuvel, E. P. J. 2001, ApJ, 546, 672

Vreeswijk, P. M., Galama, T. J., Owens, A., Oosterbroek, T., Geballe, T. R., van Paradijs, J., Groot, P. J., Kouveliotou, C., Koshut, T., Tanvir, N., Wijers, R. A. M. J., Pian, E., Palazzi, E., Frontera, F., Masetti, N., Robinson, C., Briggs, M., in 't Zand, J. J. M., Heise, J., Piro, L., Costa, E., Feroci, M., Antonelli, L. A., Hurley, K., Greiner, J., Smith, D. A., Levine, A. M., Lipkin, Y., Leibowitz, E., Lidman, C., Pizzella, A., Böhnhardt, H., Doublier, V., Chaty, S., Smail, I., Blain, A., Hough, J. H., Young, S., & Suntzeff, N. 1999, ApJ, 523, 171

Watson, D., Hjorth, J., Jakobsson, P., Pedersen, K., Patel, S., & Kouveliotou, C. 2004, A&A, 425, L33

Watson, D., Reeves, J. N., Hjorth, J., Jakobsson, P., & Pedersen, K. 2003, ApJ, 595, L29

Wheeler, J. C. & Harkness, R. P. 1990, Reports of Progress in Physics, 53, 1467

Wijers, R. A. M. J., Bloom, J. S., Bagla, J. S., & Natarajan, P. 1998, MNRAS, 294, L13

Wolf, C. & Podsiadlowski, P. 2006, `arXiv:astro-ph/0606725`

Woosley, S. E. 1993, ApJ, 405, 273

Worthey, G. 1994, ApJS, 95, 107

Yost, S. A., Harrison, F. A., Sari, R., & Frail, D. A. 2003, ApJ, 597, 459

Yun, M. S. & Carilli, C. L. 2002, ApJ, 568, 88

Yun, M. S., Reddy, N. A., & Condon, J. J. 2001, ApJ, 554, 803